

Spring 5-23-2019

Seamless Lidar Surveys Reveal Rates and Patterns of Subsidence in the Mississippi River Delta

Celeste E. Woock
cewoock@uno.edu

Follow this and additional works at: <https://scholarworks.uno.edu/td>



Part of the [Environmental Education Commons](#), [Environmental Health and Protection Commons](#), [Environmental Indicators and Impact Assessment Commons](#), [Environmental Monitoring Commons](#), [Geology Commons](#), [Geomorphology Commons](#), [Hydrology Commons](#), [Natural Resource Economics Commons](#), [Natural Resources and Conservation Commons](#), [Natural Resources Management and Policy Commons](#), [Oil, Gas, and Energy Commons](#), [Other Environmental Sciences Commons](#), [Sustainability Commons](#), and the [Water Resource Management Commons](#)

Recommended Citation

Woock, Celeste E., "Seamless Lidar Surveys Reveal Rates and Patterns of Subsidence in the Mississippi River Delta" (2019). *University of New Orleans Theses and Dissertations*. 2656.
<https://scholarworks.uno.edu/td/2656>

This Thesis is protected by copyright and/or related rights. It has been brought to you by ScholarWorks@UNO with permission from the rights-holder(s). You are free to use this Thesis in any way that is permitted by the copyright and related rights legislation that applies to your use. For other uses you need to obtain permission from the rights-holder(s) directly, unless additional rights are indicated by a Creative Commons license in the record and/or on the work itself.

This Thesis has been accepted for inclusion in University of New Orleans Theses and Dissertations by an authorized administrator of ScholarWorks@UNO. For more information, please contact scholarworks@uno.edu.

Seamless Lidar Surveys Reveal Rates and Patterns of Subsidence
in the Mississippi River Delta

A Thesis

Submitted to the Graduate Faculty of the
University of New Orleans
in partial fulfillment of the
requirements for the degree of

Master of Science
in
Earth and Environmental Sciences
Coastal and Geomorphic Studies

by

Celeste Woock

B.S. The University of Alabama, 2015

May, 2019

Acknowledgements

Louisiana's Coastal Protection and Restoration Authority through the Coastal Science Assistantship Program provided funding for this project. Louisiana Sea Grant administers the Coastal Science Assistantship Program. Both organizations are thanked for their generous support.

Table of Contents

LIST OF FIGURES.....	V
LIST OF TABLES.....	VII
ABSTRACT.....	VIII
I. INTRODUCTION	1
II. METHODS.....	4
A. LIDAR DIFFERENCE MAPS	6
1. <i>Instantaneous Slope</i>	8
B. HOLOCENE THICKNESS	9
C. OIL AND GAS WELLS.....	10
D. LEVEES.....	11
E. COASTAL PROTECTION PROJECT SITES.....	11
F. SALT DOMES.....	11
G. FIELDWORK/GROUND TRUTHING.....	11
III. RESULTS.....	14
A. RAW DATA	15
1. <i>Differenced Maps</i>	15
2. <i>Instantaneous Slope Maps</i>	16
B. ANCILLARY DATA WITH RAW DATA.....	21
1. <i>Holocene Thickness</i>	21
a. Raw data.....	21
b. Processed data.....	21
C. ANCILLARY DATA WITH DIFFERENCE MAPS.....	21
1. <i>Oil and Gas Wells</i>	22
a. Hundreds of Kilometers Scale	22
b. Tens of Kilometers Scale	23
c. Kilometer Scale.....	23
2. <i>Levees</i>	26
a. Hundreds of Kilometers Scale	26
b. Tens of Kilometers Scale	27
c. Kilometer Scale.....	28
3. <i>Coastal Protection Project Sites</i>	32
a. Hundreds of Kilometers Scale	32
b. Tens of Kilometers Scale	32
c. Kilometer Scale.....	35
4. <i>Salt Domes</i>	37
a. Hundreds of Kilometers Scale	37
b. Tens of Kilometers Scale: Bully Camp and Leeville	37
c. Kilometer Scale: Clovelly and Venice	39
IV. DISCUSSION	41

A. SUBSIDENCE	41
1. <i>Rate variability and inherent error.....</i>	43
2. <i>Near Surface Processes.....</i>	43
3. <i>Deep fluid withdrawal, oil and gas.....</i>	43
4. <i>Salt Domes.....</i>	44
5. <i>Thickness of the Holocene</i>	45
B. ACCRETION	45
1. <i>Coastal Protection Project Sites.....</i>	45
2. <i>Accretion associated with sediment transport from the Mississippi River</i>	46
C. EROSION.....	47
V. CONCLUSION.....	48
VI. REFERENCES	50
VII. APPENDIX A: TABLES	56
VIII. APPENDIX B: SUPPLEMENTAL FIGURES	61
IX. VITA	63

List of Figures

Figure 1	2
Figure 2	2
Figure 3	3
Figure 4	4
Figure 5	5
Figure 6	6
Figure 7	7
Figure 8	8
Figure 9	9
Figure 10	10
Figure 11	16
Figure 12	17
Figure 13	18
Figure 14	19
Figure 15	20
Figure 16	21
Figure 17	22
Figure 18	23
Figure 19	24
Figure 20	27
Figure 21	28
Figure 22	29
Figure 23	30
Figure 24	31
Figure 25	31
Figure 26	32
Figure 27	32

Figure 28	33
Figure 29	34
Figure 30	35
Figure 31	36
Figure 32	37
Figure 33	38
Figure 34	39
Figure 35	40
Figure 36	41
Figure 37	61
Figure 38	61
Figure 39	62

List of Tables

Table 1	56
Table 2	57
Table 3	59
Table 4	14

Abstract

Light Detection and Ranging (Lidar) data are used to report the temporal and spatial patterns of subsidence as well as the potential contributors to subsidence within the Barataria and Terrebonne Bays. In recent decades, subsidence in southeast Louisiana has become a topic of substantial and growing concern to the scientific community, the local residents, and all those invested in the region. Lidar data were acquired from the United States Geological Survey (USGS) and the LSU Center for Geoinformatics. The data has been manipulated to map the differenced Lidar, complete an instantaneous slope analysis, and determine the thickness of the Holocene sediments. The goal was to gain a more comprehensive understanding of the subsidence patterns and the dynamic processes driving subsidence within the study area. These efforts provide a better ability to plan for the future of the Louisiana working coast and mitigate against relative sea level rise and coastal land loss.

Keywords: Lidar, subsidence, land loss, relative sea level rise, Mississippi River Delta

I. Introduction

Subsidence in the Mississippi River Delta is a significant problem. It contributes to land loss, lower elevation of infrastructure such as levees and, along with global sea level rise it adds to relative sea level rise and an increase in coastal flooding. Despite the clear importance of understanding subsidence, the scientific community still has questions about subsidence rates, spatial and temporal variability in these rates, and the underlying geological and anthropogenic factors driving subsidence.

Land loss in the Mississippi River Delta Plain is an issue that has been of considerable concern and has been escalating for more than a century (Alexander et al., 2012). The disconnect between the Mississippi River's main channel and its distributary network due to damming and the building of levees is one of many variables contributing to land loss in the deltaic region (Alexander et al., 2012). Up-river damming causes the base level of the river to adjust in such a way that base discharge is increased downstream while the overall variability of river discharge is lessened (Alexander et al., 2012). Artificial levees inhibit overbanking, which, in turn causes a lack of sediment introduced from the river to the delta plain during flood events (Kesel, 1988). The Mississippi River provides to the delta plain only 30 % of the sediment load it carried in 1850 due to revetments, dikes and large reservoirs, and changes in agricultural practices (Kesel, 1988). Some of the foremost implications of this include a: (1) loss of elevation of channel-bed boundary; (2) loss of channel dynamism; and (3) loss of interaction between the primary river channel and its distributary network (Alexander et al., 2012). Loss of sediment load is a large factor in land loss in the Mississippi River Delta. Additionally, subsidence also contributes significantly to land loss in the coastal region.

Subsidence in coastal Louisiana is the result of many mechanisms and many of the subsidence processes began before the delta was settled (Figures 1 & 2) (Yuill et al., 2009). However, the problem has been exacerbated since human engineering began in the Mississippi River Delta and sea level rise began to increase (DeLaune and Pezeshki, 1994). Concerns are growing due to the recent record magnitude of subsidence rates documented for many areas of Louisiana's coastal zone. Subsidence has the potential to impose serious damage to coastal wetlands, cities, infrastructure, wildlife habitats and agricultural regions (Shinkle & Dokka, 2004).

Faulting, Forebulge Collapse, and Compaction

Faulting has been implicated to have an effect on subsidence rates and patterns across southeast Louisiana (Gagliano et al., 2003a; Dokka, 2006). Through parts of the Cenozoic, the uplift and formation of the Rocky Mountains during the Laramide orogeny provided sediment to coastal regions as river systems formed (Dokka, 2006). This led to the rapid progradation of the northern Gulf margin. Because of this, much of the Mississippi River Delta's underlying strata is

tectonically unstable (Dokka et al., 2006; Tornquist et al., 2008). The instability is exacerbated by the relative buoyancy of the underlying Jurassic salt horizons (Yuill et al., 2009).

Many studies suggest that salt migration and fault movement within the region cannot be ignored when considering the patterns of subsidence (e.g. Morton et al., 2005; Armstrong et al., 2014; Dokka, 2006; Dokka et al., 2008; Gagliano et al., 2003a). As the buoyant salt intrudes upward through the deltaic sediment strata, it causes an increase in local pressure gradients, which can lead to fault movement in existing fault zones (Diegel et al., 1995). Additionally, radial faults form around the salt diapirs, increasing the concentration of faults in these areas.

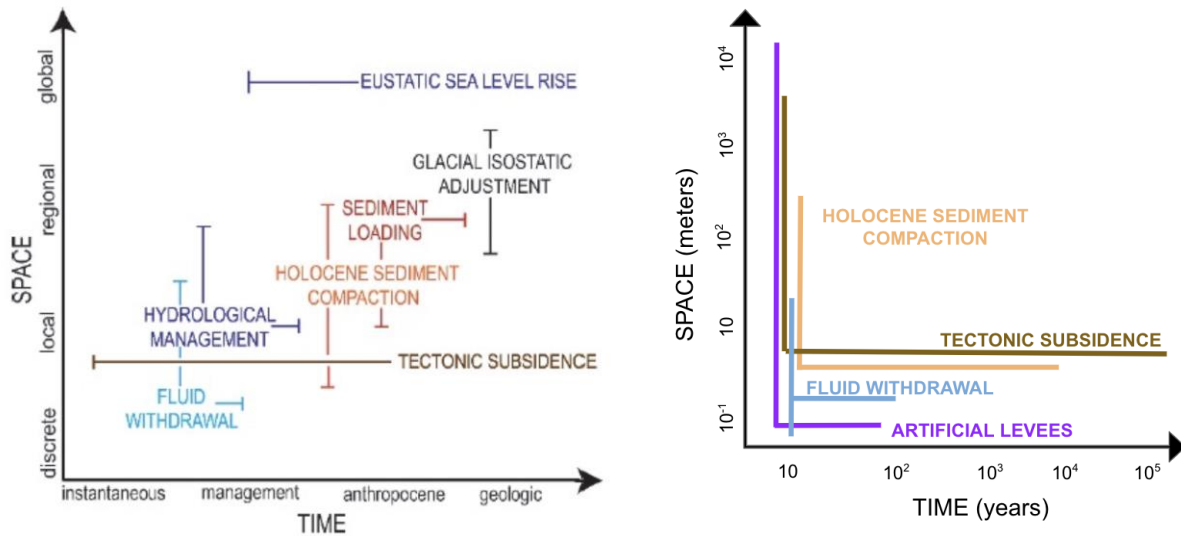


Figure 1: Original graphic from Yuill (2009) plotting the spatial and temporal ranges of subsidence contributors. The time ranges are quantified as follows: instantaneous includes 0–1 year, management includes 1–20 years, anthropocene includes 20–400 years, and geologic ranges at least 400 years (Yuill et al., 2009).

Figure 2: A modified version of the Yuill graphic reflecting the observations anticipated by this study during the hypothesis phase. A logarithmic scale is used for temporal and spatial ranges.

The impact of faulting is sometimes visible at the surface in wetlands due to increased subsidence on the hanging wall side (hanging wall side will be inundated). River channels will also tend to follow the strike on the hanging-wall side of growth faults due to the increased subsidence (Armstrong et al., 2014; Gagliano et al., 2003b).

Instability of much of the Cenozoic strata in the region originated prior to the growth of the Holocene delta, however, following the retreat of the Laurentide ice sheets, the Gulf Coast experienced ice-sheet forebulge collapse (Törnqvist et al., 2012). Though the resulting lithospheric flexure may continue for millennia, the effect of this is several orders of magnitude smaller than that of lithospheric flexure due to sediment loading (Yu et al., 2012).

Faulting and forebulge collapse are processes that control regional land elevation changes. More small-scale processes may control subsidence on the horizontal scale of meters or kilometers and exist closer to the land surface. Near surface processes involve high rates of

immediate subsidence, especially within peat layers. Peat horizons have been analyzed to determine the rate at which they compact. Typically, the majority of peat compaction due to physical and biological processes occurs relatively quickly (within 100-1000 yr) initially, but on the millennial scale, compaction rates average 5 mm/yr (Törnqvist et al., 2008). This implies that Holocene sediment compaction is a sizeable contributor to local subsidence, wetland loss and relative sea level rise (RSLR) (Törnqvist et al., 2008).

Study Area

The focus of this research is on two areas, Terrebonne and Barataria. The Terrebonne data covers most of Terrebonne Parish. In the west, it extends from Morgan City to Cocodrie but excludes some of the Terrebonne Bay marshland. All of the barrier islands south of Terrebonne Parish are excluded. The Barataria data covers parts of Lafourche, Jefferson and Plaquemines Parishes. The Barataria data includes the barrier islands and extends east to the Mississippi River and south to Venice (Figures 3 & 4).

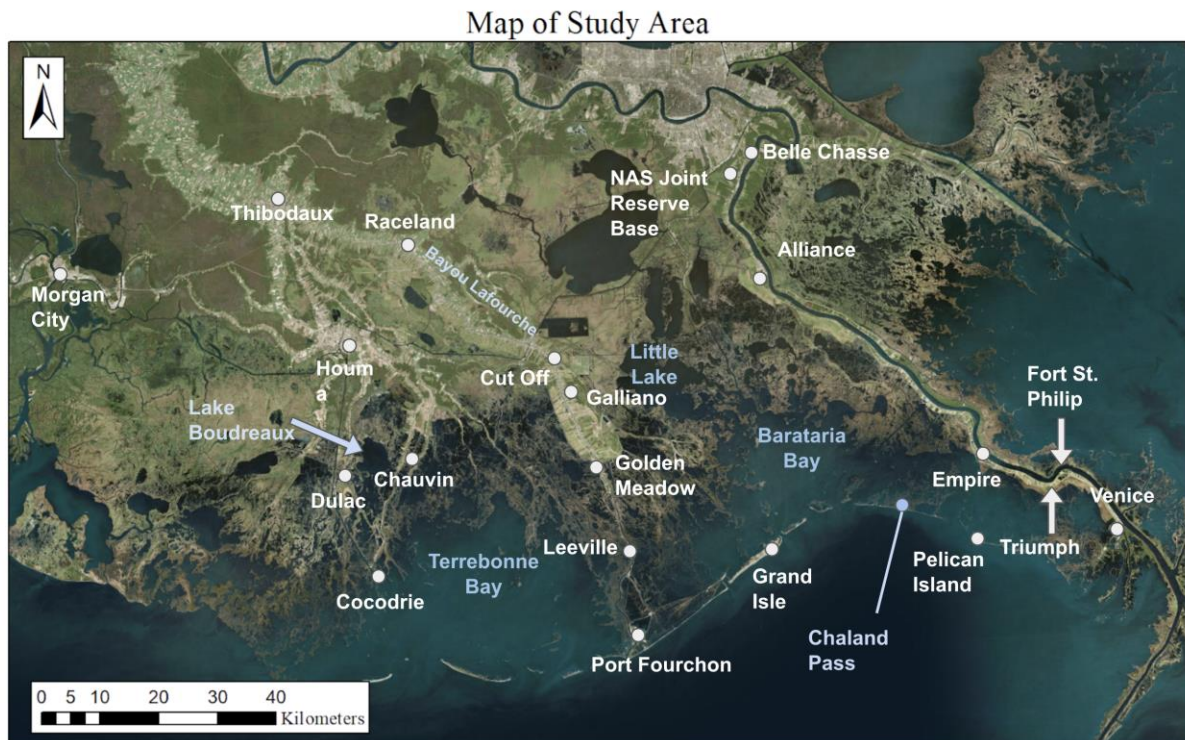


Figure 3: Map of south central coastal Louisiana showing the areas of study and place names that are referred to in the text.

Study Area

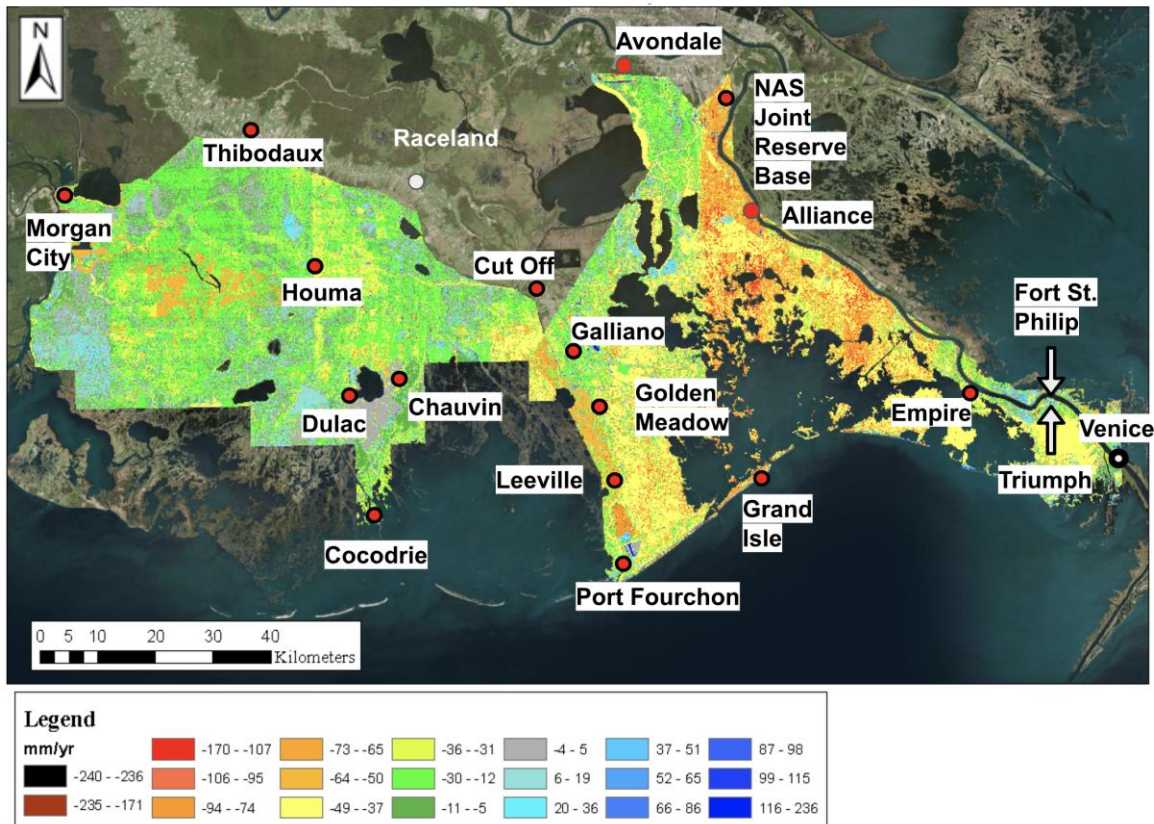


Figure 4: Map of study area showing the distribution of Lidar data used in this study. Warm colors indicate subsidence (reds and oranges), whereas and cooler colors such as greens and blue indicate accretion.

Objective

The objective of this study was to develop a high resolution map of subsidence for targeted areas in coastal Louisiana, and to use this map to help inform a better understanding of the processes that drive subsidence in coastal Louisiana.

Hypothesis

Across decades and tens of kilometers, the primary drivers of subsidence are regional faulting, fluid withdrawal, and the impacts of impoundments on near surface sediment compaction.

II. Methods

For this study, Lidar data were gathered and then manipulated with ancillary datasets to determine trends and patterns of subsidence. The Lidar were collected from an array of sources

(e.g. USGS and LOSCO) and processed with ArcGIS 10.3.1. Table 1 provides specifications on each dataset including their spatial resolution. The units of z values, geoid and datum were all made congruent for ease of processing. A GIS layer package from 2007 Louisiana Coastal Marsh-Vegetative Type Map of the Louisiana Coastal Marsh-Vegetative Type Database was used to mask out significant water bodies from generated map that was generated. Following initial processing, the USGS (2013/2015) and LOSCO (2002/2003) Lidar datasets were differenced (Figures 5 & 6). The differenced map was adjusted mathematically to render subsidence rate (mm/yr) maps for the approximate given time period (Figure 8).

Raw LOSCO Lidar Data

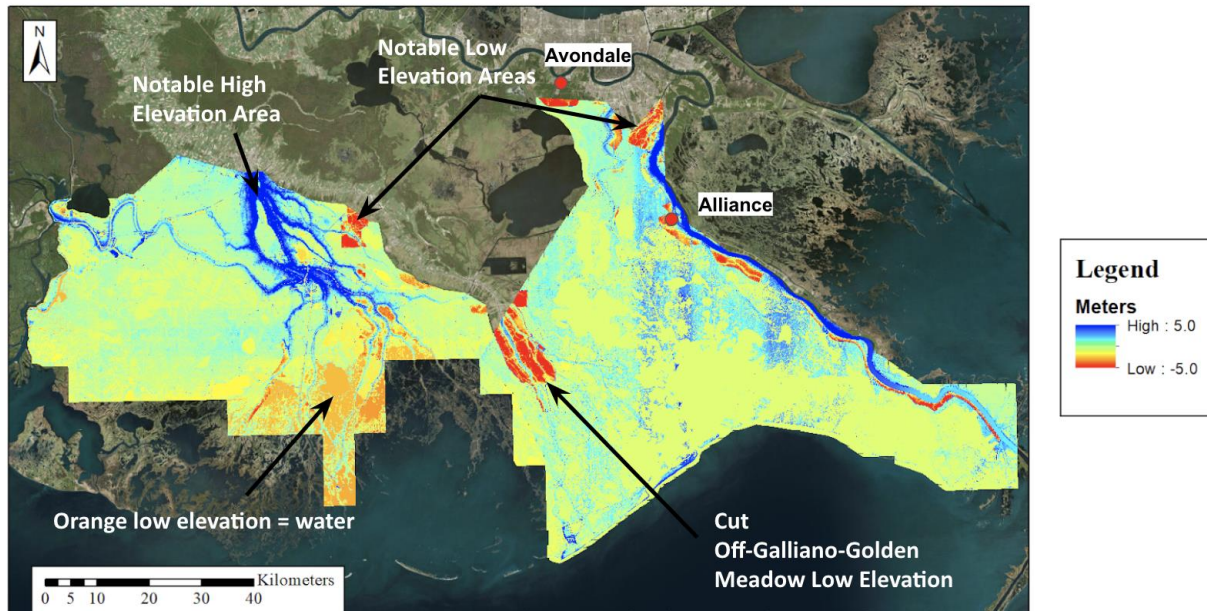


Figure 5: Seamless LOSCO Lidar data, adjusted to datum and units made congruent (metric) to other datasets; Homogeneously colored areas indicate water bodies; A vertical swath error is present in the center of the Barataria data, identified by the south-trending lineation of blue colors.

A Holocene thickness map was created to determine if the thickness of the Holocene is a control of subsidence within the study area. A map of the Holocene-Pleistocene Boundary (Holocene Surface Isopach Map, 2013) was obtained from CPRA. The thickness map was created by differencing the Holocene-Pleistocene contact elevation raster from the LOSCO and USGS surveys. Point values from the resulting Holocene thickness maps were then plotted

against those of the subsidence rate map to identify any potential trends.

USGS Raw Lidar Data (2013/2015)

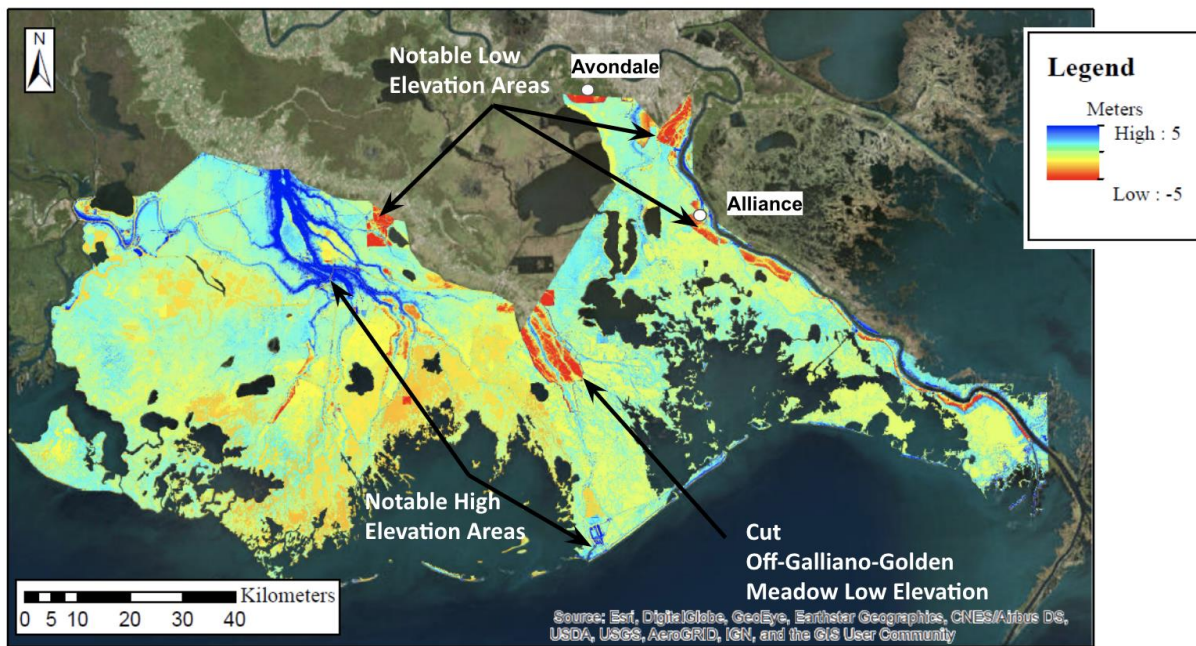


Figure 6: Raw USGS Lidar data shows areas of high elevation in cool colors and areas of low elevation in warm colors; large water bodies were extracted from the original data.

Shapefiles of oil and gas wells, injections wells, levees, salt domes, faults and coastal restoration project sites were cross-referenced with the subsidence rate map to determine correlations between each feature set and associated anomalous subsidence rates. See Table 1 for specifics of the datasets acquisition.

All of these data have sources of uncertainty including, but not limited to: path of the plane while in flight (variations in vertical distance from land surface), correction algorithm errors, discrepancies between the datum and time the data were collected, and inherent precision value of the Lidar. Additionally, in many areas the water could not be extracted from the map and is instead displayed as values ranging from -8.1 to -1.5 m in the finalized maps. The results assume a constant rate of change during the time interval of the study (2002/2003 - 2015) on a mm/yr observational scale.

A. Lidar Difference Maps

The LOSCO Lidar was acquired as a seamless raster of Digital Elevation Model (DEM) files. For accurate processing, the seamless Lidar was separated by the acquisition date of the

individual Digital Elevation Model (DEM) files (Figure 7).

LOSCO Acquisition Dates

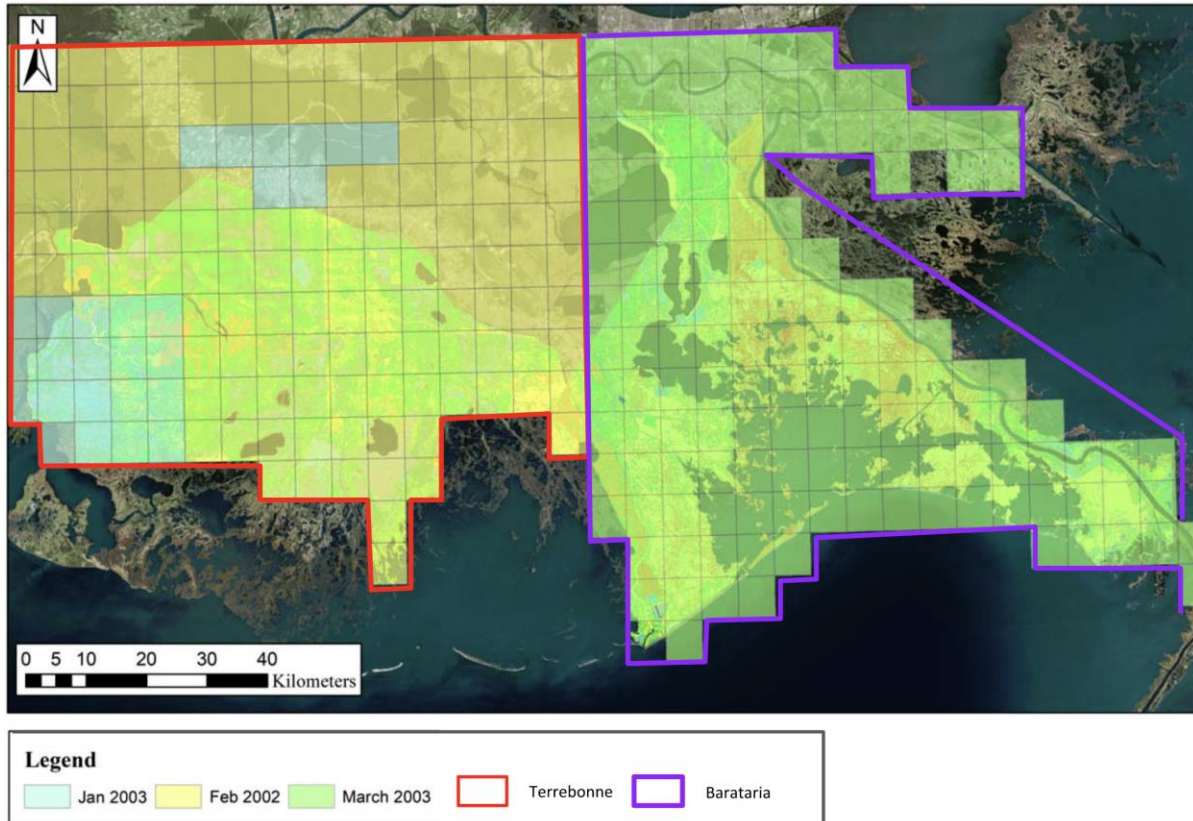


Figure 7: LOSCO data was acquired in parts during February 2002, January 2003 and March 2003; Barataria data was collected entirely in March 2003 and Terrebonne data was collected in February 2002 and January 2003.

The majority of these data were collected during February of 2002 for Terrebonne Basin, with additional acquisition occurring in February of 2003. Each difference map combined several datasets, consisting of a number of DEMs, which were collected concurrently within 1 year (Figure 7). A list of the merged datasets, and their acquisition properties is presented in Table 1. An accurate subsidence rate was determined by using the acquisition date of each DEM while differencing the Lidar datasets. The LOSCO Lidar in Barataria were entirely shot in 2003 (Figure 7). The USGS Terrebonne (2015) and Barataria (2013) datasets were then differenced from the LOSCO 2002/2003 data.

Subsidence Map

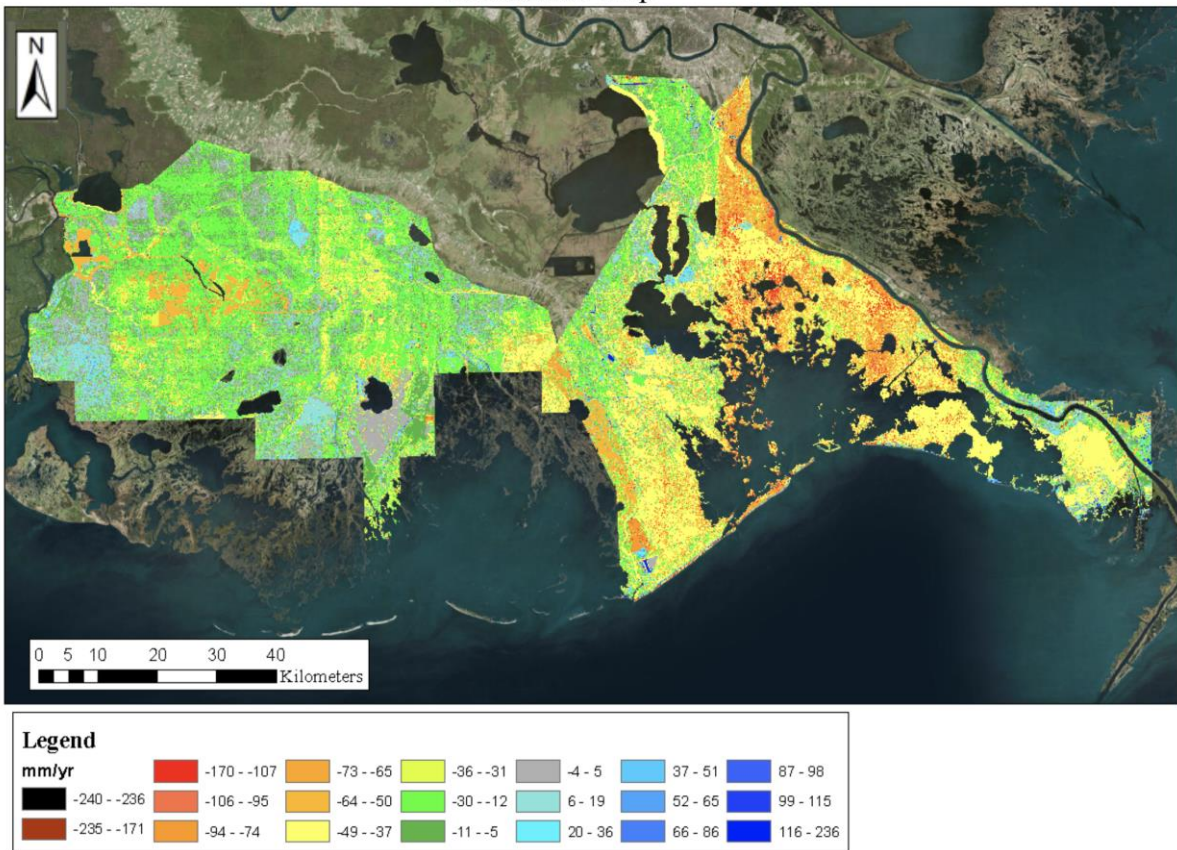


Figure 8: Following initial processing, the USGS (2013/2015) and LOSCO (2002/2003) Lidar datasets were differenced; the differenced map was adjusted mathematically to give subsidence rate (mm/yr) maps for the given time period.

1. Instantaneous Slope

The instantaneous slope of the LOSCO Lidar and USGS Lidar dataset were calculated and differenced in order to determine potential causes of elevation change in a given area or region. The instantaneous slope for each data set was derived from elevation values using the Slope tool in ArcMap 10.3. The slope is utilized to measure if subsidence controls in a given area are regional or more precisely concentrated. The “Slope” feature in ArcGIS 10.3.1 Spatial Analyst - Surface feature set was used to determine the instantaneous slope of the differenced LOSCO Lidar and USGS Lidar. The “Slope” tool “identifies the slope (gradient or rate of maximum change in z-value) from each cell of a raster surface.”

Instantaneous Slope map of Barataria = Instantaneous slope of LOSCO Lidar -
Instantaneous slope of USGS Barataria Lidar

and

Instantaneous Slope map of Terrebonne = Instantaneous slope of LOSCO Lidar -
Instantaneous slope of USGS Terrebonne Lidar

B. Holocene Thickness

The Coastal Protection and Restoration Authority (CPRA) created the Holocene surface isopach map in 2013 through the collection and analysis of hundreds of cores (Heinrich, et al., 2015). The Holocene-Pleistocene surface was created using the Spline with Barrier Interpolation method. Using these data, maps were made of the Holocene thickness for the Barataria 2013 and Terrebonne 2015 Lidar datasets. The purpose of the extraction of the thickness between the Holocene base and modern land surface was to examine whether there exists a correlation between Holocene thickness and subsidence rates determined from the Lidar data.

Holocene-Pleistocene Boundary Surface Raw Data

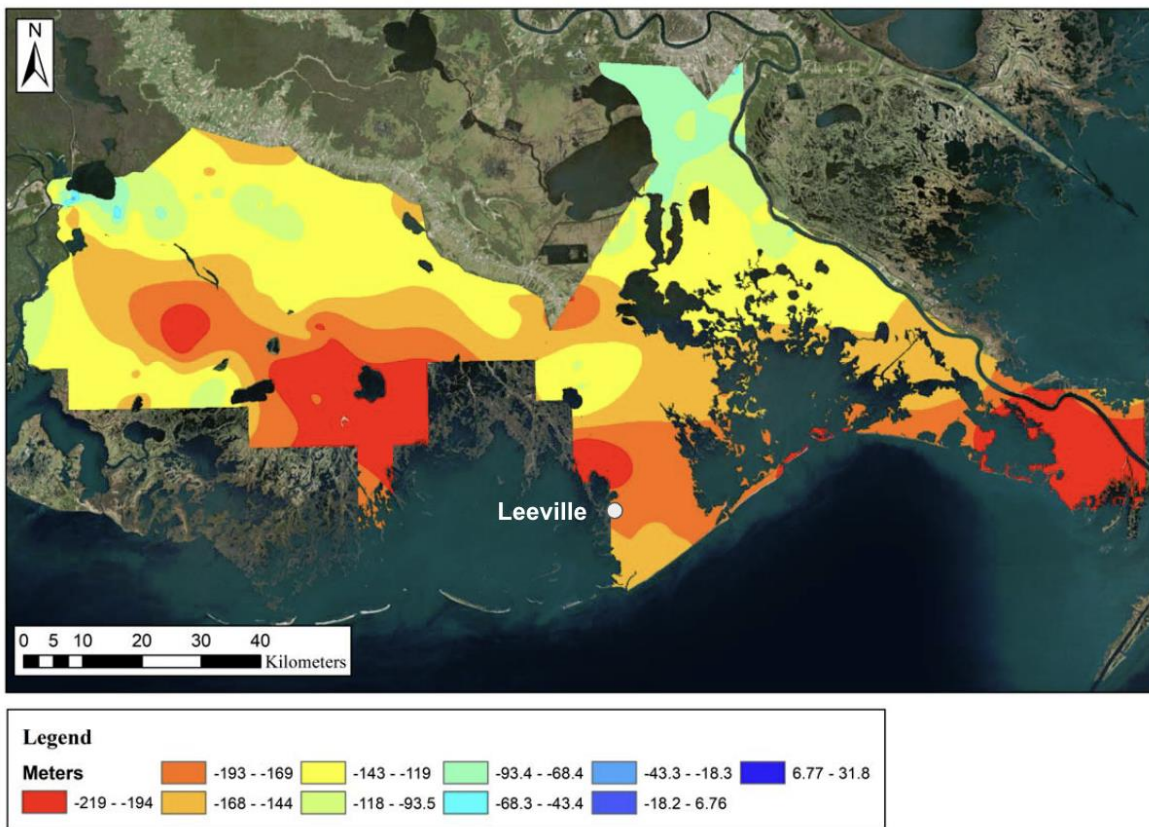


Figure 9: Structure contour showing the depth to the Holocene-Pleistocene Boundary but clipped to the data frame and with water extracted (map data from Heinrich, et al., 2015).

To do this, sections (or, raster clips) were made of each section of the Holocene-Pleistocene boundary raster that corresponded with the USGS_Bara_2013, USGS_Terre_2015 and USGS_NBara_2013 data. These were differenced in order to create a cohesive map. Then, the USGS_Bara_2013, USGS_NBara_2013, and USGS_Terre_2015 data were subtracted from their respective sections of the Holocene-Pleistocene boundary raster (“hp_surfacel” raster). This

created a difference between the two surfaces, which serves as the approximate thickness of the Holocene.

Depth to Holocene-Pleistocene Surface from LOSCO Lidar

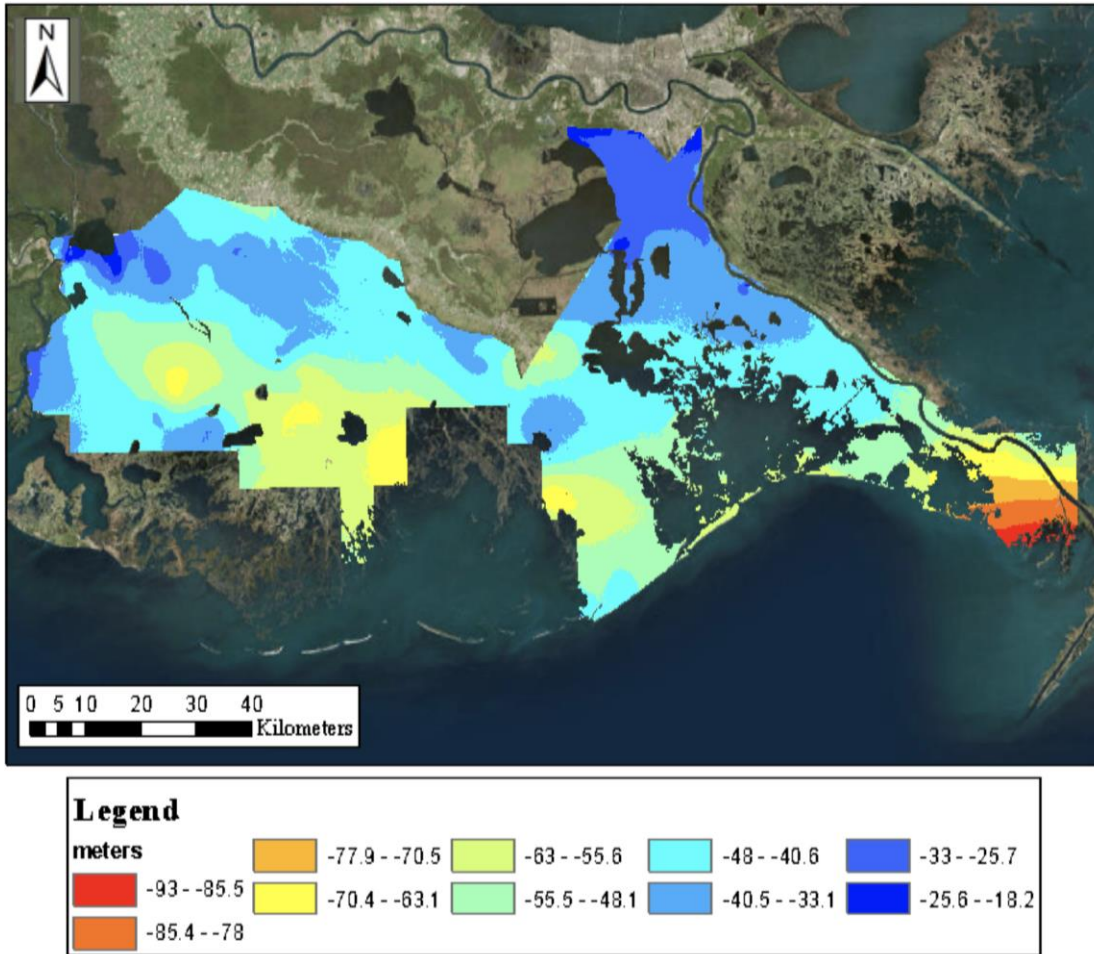


Figure 10: The depth to the Holocene-Pleistocene Boundary map shows that the Holocene is thickest near the mouth of the Mississippi River, where the depth to the Holocene-Pleistocene boundary can be as much as -93 m; The Holocene is also thick near Cutoff and central Terrebonne where depths to the boundary approach 70 m.

The formula is as follows:

Holocene surface clipped raster – USGS_Bara_2013 clipped raster = Holocene thickness map

This process was repeated with the USGS_Terre_2015 and LOSCO_Bara_2002/3 data.

C. Oil and Gas Wells

Shapefiles of oil and gas well sites in addition to injection well site locations were overlain on the difference maps. These data were acquired through the Louisiana Department of Natural Resources (LDNR) public access Strategic Online Natural Resources Information System (SONRIS) database.

D. Levees

Louisiana levee system shapefiles were also acquired through the LDNR public access SONRIS site. These were then compared with the difference maps to determine general trends in land elevation change on either side of an engineered levee system during a given time period. Additionally, several areas were analyzed to determine more precise cause and effect relationships between the levees and notable changes in land surface elevation.

E. Coastal Protection Project Sites

A shapefile containing detailed information on coastal restoration projects was acquired through the LDNR public access SONRIS database. These sites were studied simultaneously with the difference maps to determine if any elevation changes have occurred near already constructed projects or what the general trend of elevation change is in proposed project sites.

F. Salt Domes

Salt dome and fault location data was cross-referenced with the subsidence rate to determine if there were linkages between salt domes and subsidence. The fault map was obtained from Nancye Dawers (pers. comm), and has been presented in Dawers et al., (2017).

G. Fieldwork/Ground Truthing

Fieldwork was completed to ground-truth the Lidar data and examine notable areas of significant subsidence rates. Real-Time Kinematic (RTK) Rover data were gathered at these sites and compared to calculated subsidence rate values and raw data measurements. RTK data has a greater accuracy that is more reliable than broad-scale Lidar because of fewer variables. The precision for RTK data is <1 cm for 3 minute points and <3 cm for instantaneous points. For this study, instantaneous point measurements were used. These data were gathered July 29, 2017 using RTCM_IMAX reference. Data was collected from areas near Chauvin, Port Fourchon and Dulac, and are listed in full in Table 4. Trimble R8 RTK GPS Rover Station was used to gather real time GPS Points in the following areas of interest:

1. Leonard's Property
2. Chauvin
3. Port Fourchon

The RTK data from the Chauvin site were taken along the levee just west of the West Lake Boudreaux Shoreline Protection and Marsh Creation Project (CWPPRA) (Figure 31 and 31b). Just northeast of the western levee, high subsidence rates were concentrated near a pasture where water was being pumped from the pasture to the other side of the levee (Appendix B, Figure 38). The removal of surficial water may account for the elevation loss rates exceeding -240 mm/yr.

These ground-truthed values indicate the Lidar data to be adequately precise for the purposes of this study as all values for the USGS data were <0.26 m off from the GPS/RTK values. The difference between the GPS determined elevation and the LOSCO Lidar determined elevation ranged from 0.331 to -2.40 m, and averaged -0.671 m. The difference between the GPS and the USGS Lidar ranged from 0.251 to -0.023 m, and averaged 0.117 m. Difference between GPS determined elevations and either Lidar dataset determined elevations appear to be associated with the construction of levees.

Fieldwork area	Latitude	Point #	2016 GPS/RTK Measurement (m)	LOSCO value (m)	Terrebonne Value (m)	Differenced Lidar Value (m)	Calculated Diff b/w LOSCO and GPS value (m)	Difference b/w Terrebonne and GPS/RTK measured value (m)
Leonard's Property	90°35'4.9"W 29°28'59.211" N	A117	1.398 (top of levee)	1.615	1.459048	-0.2128	0.217	0.061
Leonard's Property	90°35'4.9"W 29°28'59.211" N	A118	-0.6556 (bottom of ditch)	-0.9144	-0.5698	0.3744	-0.2558	0.0858
Chauvin	90°41'55.775" W 29°26'22.54" N	A119	1.433 (top of levee, next to pump)	0.4877	1.410	0.4594	-0.9453	-0.023
Chauvin	90°41'55.775" W 29°26'22.54" N	A120	0.7264 (basin side of levee)	0.6401	0.9647	0.7778	-0.0863	0.2383
Chauvin	90°41'55.775" W 29°26'22.54" N	A121	0.06485 (cow farm side of levee)	0.3962	0.3155	0.5650	0.3314	0.2506
Chauvin	90°41'55.775" W 29°26'22.54" N	A122	-0.0217 (outside of levee)	-0.3048	0.0640	0.3834	-0.2831	0.0857
Chauvin	90°41'55.775" W 29°26'22.54" N	A123	2.098 (top of levee)	-0.3048	2.145	2.448	-2.4028	0.0470
Chauvin	90°41'55.775" W 29°26'22.54" N	A124	0.4224 (basin side of levee)	-0.3048	0.6145	1.627	-0.7272	0.1921
Port Fourchon	90°12'0.219" W 29°8'16.474"N	A125	1.080 (construction area)	0.0914	No data	No data	-0.9886	No data
Port Fourchon	90°12'0.219" W 29°8'16.474" N	A126	1.658 (road)	0.0914	No data	No data	-1.567	No data

Table 4: Compiled RTK Fieldwork/Ground-truthing data; Points A119, A120, A121, A122, A123, A124 are associated with the West Lake Boudreaux Shoreline Protection and Marsh Creation Program; points A117 and A118 were taken at the Leonard's Property site, adjacent to an old levee system, which extended inland from Lake Boudreaux and a newer levee which cut off the old levee inland section; points A125 and A126 were taken at Port Fourchon nearby a newly constructed parking lot.

The Leonard's Property site is adjacent to an old levee system - which extended inland from Lake Boudreaux – and a newer levee that cut-off the old levee inland section. The Chauvin site is associated with the West Lake Boudreaux Shoreline Protection and Marsh Creation Program.

Additionally, a flight over the study area was completed in order to observe areas of interest more closely and therefore aid in the understanding of the processes affecting the study area. It also served to allow visual verification of anomalous rates within inaccessible areas.

III. Results

Figure 5 is an elevation map of coastal Louisiana developed using data from the LOSCO sources from the 2002-2003-acquisition period (dataset LOSCO_2002/3). This map shows areas of high elevation in cool colors and areas of low elevation in warm colors. The LOSCO Lidar dataset has a horizontal resolution of 5 m. The vertical precision of the raw point data is 0.15 to 0.30 m (6 to 12 inches) and horizontally between 0.91 to 1.8 m (3 to 6 ft). Point spacing is every 4 m in phase 1 of data collection and 3 m in stage 2. In the raw data the vertical value or elevation in meters is relative to the datum, NAD83. Overall, elevations in coastal Louisiana ranged from -5.2 to 15.8 m, with 95% of values in the range of -0.27 to 0.77 m assuming a normal distribution. Example areas of low elevation include inside the Cutoff-Galliano-Golden Meadow Leveed Area (CGGM), an area just south of Raceland, around Belle Chasse the leveed area around the NAS Joint Reserve Base and in barrier island overwash areas. The Bayou Lafourche floodplain near Thibodaux is generally of higher elevation than surrounding areas (Figure 6).

Figure 6 is an elevation map of coastal Louisiana developed using data from the 2013 and 2015 USGS data (datasets USGS_Terre_2015, USGS_NBara_2013, USGS_Bara_2013) (Figure 6). This map shows areas of high elevation in cool colors and areas of low elevation in warm colors. Overall, elevations in coastal Louisiana ranged from -3.04 to 3.07 m, with 95% of values in the range of -1.06 and 0.68 m assuming a normal distribution. Outliers such as levees can be 9 to 25 m in height. Examples areas of low elevation include the leveed areas near the Mississippi River at Alliance, and the CGGM. The highest elevations are in the Bayou Lafourche floodplain and the developed areas around Port Fourchon.

Figure 8 is a difference map of coastal Louisiana developed using data from the USGS and LOSCO Lidar sources (datasets USGS_Terre_2015, USGS_NBara_2013, USGS_Bara_2013 and LOSCO_2002/3). This map shows areas of high subsidence in warm colors and areas of accretion in cool colors. Overall, subsidence rates in coastal Louisiana ranged from -170 to 51 mm/yr, with most values in the range of -30 to -12 mm/yr. Areas with the highest subsidence rates include marsh edges in cusps and bays, inland marshes and overwash areas of barrier islands. Land elevation gain is observable at project sites, such as the Little Lake Shoreline Protection marsh creation project; the Barataria Basin landbridge dedicated dredging area and large-scale marsh creation (NRDA), and near the Mississippi River at Triumph.

A. Raw Data

Several key features are observable in the raw LOSCO Lidar dataset. Low elevations are observed inside the CGGM leveed area, south of Raceland, around Belle Chasse/ the leveed area around the NAS Joint Reserve Base, leveed areas on the west side of the Mississippi River and in barrier island overwash platforms. Within the CGGM leveed area, elevations range from -0.30 to -1.25 m, with the highest closest to Bayou Lafourche. Another example of marked low elevation is the area just south of Raceland where elevations range from -0.5 to -1.46 m. Higher elevations are present in the Bayou Lafourche floodplain near Thibodaux with elevations ranging from around 2.2 to 3.4 m.

In the USGS Terrebonne and Barataria data (Figure 6), all of the notable areas of high and low elevations from the LOSCO Lidar are the same. Some of the lowest elevations are found within the CGGM levee system, the leveed area near Alliance and the area just south of Raceland. The most marked change between these data and the LOSCO Lidar are the higher elevation values found on barrier islands. Segments of barrier islands - particularly Grand Isle - have clear positive elevation values of ~ 0.31 to 1.5 m. The developed areas near Port Fourchon give a good indication of how higher elevation developed areas appear in the data. Some of the highest elevations within the dataset are in Port Fourchon and are as much as 1.75 m.

1. Differenced Maps

Table 3 identifies the raw datasets that were used to create the differenced Lidar maps, which identify the rate of elevation change between the 2015 Terrebonne and LOSCO Lidar as well as the 2013 Barataria and LOSCO Lidar (Figure 8).

Figure 8 shows the differenced Lidar map. Land elevation changes of -170 to -50 mm/yr along marsh edges of bays, cusps, and lakes are represented by the differenced Lidar map of Figure 11. Inland marshes near Lake Boudreaux, Little Lake and the sulfur mining area west of Galliano all show high subsidence rates, typically between -50 to -94 mm/yr. Barrier island overwash areas are another notable high subsidence area - particularly on Grand Isle where can be as much as -150 mm/yr.

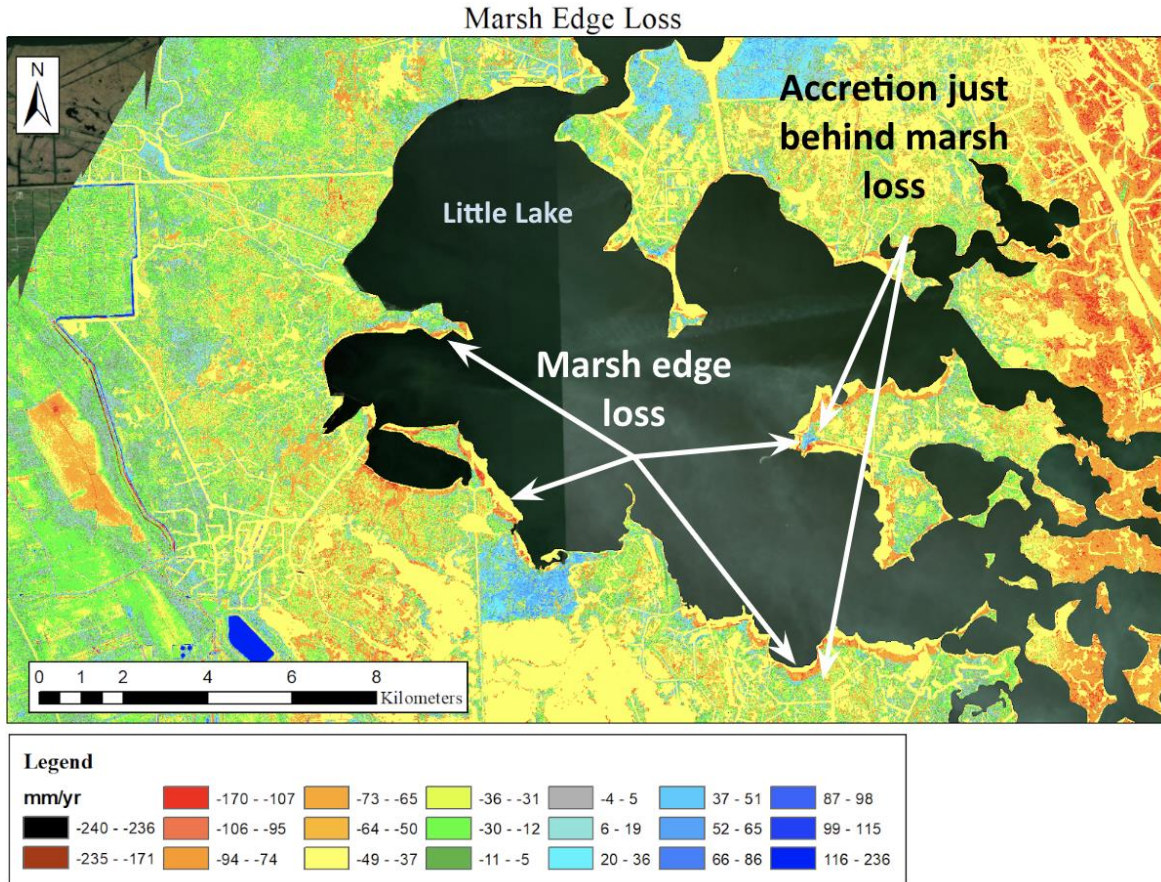


Figure 11: Subsidence rates over -50 mm/yr line the cusps and shorelines of Little Lake; there is slight accretion behind the shore edge, which could be indicative of something like a barrier island rollover effect.

The positive land elevation gain at project sites, such as the Little Lake Shoreline Protection marsh creation project is apparent (Figure 29). At this site, apparent accretion rates range from 37 to 100 mm/yr. Overall, the Terrebonne Bay is undergoing more positive rates of land elevation change than Barataria. Accretion values near the Mississippi River at Triumph range from 20 to 50 mm/yr with some outlier values, which reach 80 mm/yr.

Due to a data processing error in the original data, much of the eastern portion of the Barataria data is skewed. The error follows a clearly defined north trending line and seems to be a result of incorrect calibration of the Leica Geosystems ALS40 LIDAR mapping system for the swath of anomalous Lidar. It also could be the result of a miscalibration or miscalculation by the software or algorithm involved in immediate data processing (ELVIS software). Despite this, conclusions regarding relative rates of change on the m-scale may still be made. Additionally, hydroflattening errors occur within large bodies of water, but subsidence rates within water bodies are not measurable using Lidar - making these anomalies inconsequential for this study.

2. Instantaneous Slope Maps

The instantaneous slope map (Figure 12) is used to observe the rate of change of the subsidence during a specified time period (dip magnitude or slope). A high slope value corresponds to more variability in elevation of the area. A fixed area of marsh with a drop off of ~15.2 cm (6 in) to water level would have a relatively high instantaneous slope value. This is because the change in the slope occurs drastically from the elevation of the top of the marsh to the elevation of water level. The same size area on the side of a sand dune or hill would have a relatively low slope value. A low value in the output raster corresponds to low variability of elevations in the area. An area that is particularly flat or smooth, such as a parking lot or beach, will have a much lower instantaneous slope value than marshland or forest.

Instantaneous Slope Map

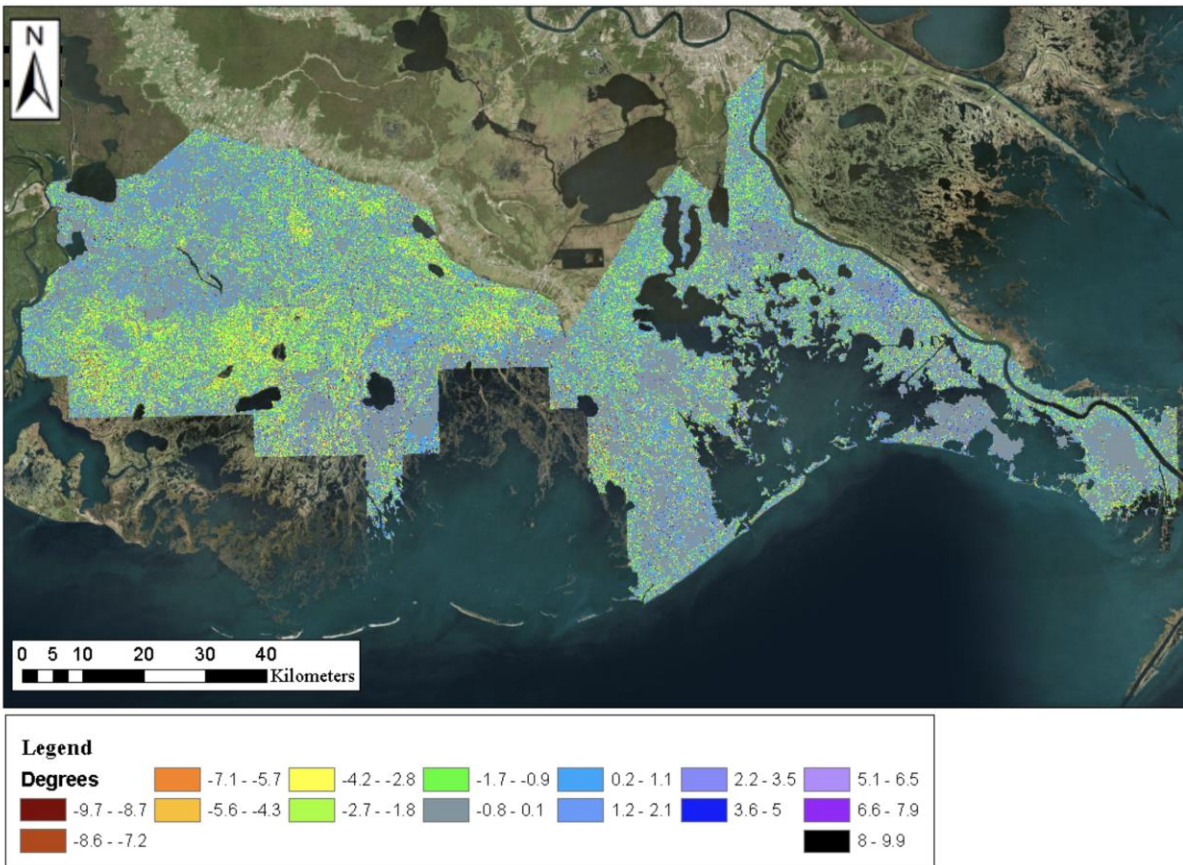


Figure 12: This map is the result of subtracting the 2013/15 USGS slope map from the 2002/3-slope map. This was done to observe the rate of change of the subsidence during the specified time period. A high slope value corresponds to more variability in elevation of the area. A low value in the output raster corresponds to low variability of elevations in the area. Values near zero indicate little to no change in geologic processes over the time period.

Positive slope values may correspond with decreasing rates of subsidence/land loss or water inundation on cusps and shorelines (Figure 14). These positive values specifically show the effect of depositional processes, seasonal erosion or short-term subsidence patterns. Negative values correspond with increasing rates of subsidence, likely due to regional contributors, such as differential subsidence, fault motion and halokinesis. Short-term subsidence contributors have a larger effect in the study area than regional components. At the hundreds of kilometers scale,

slope values of ~ -4.2 to -0.9° are concentrated in the central-southwestern portion of the Terrebonne dataset.

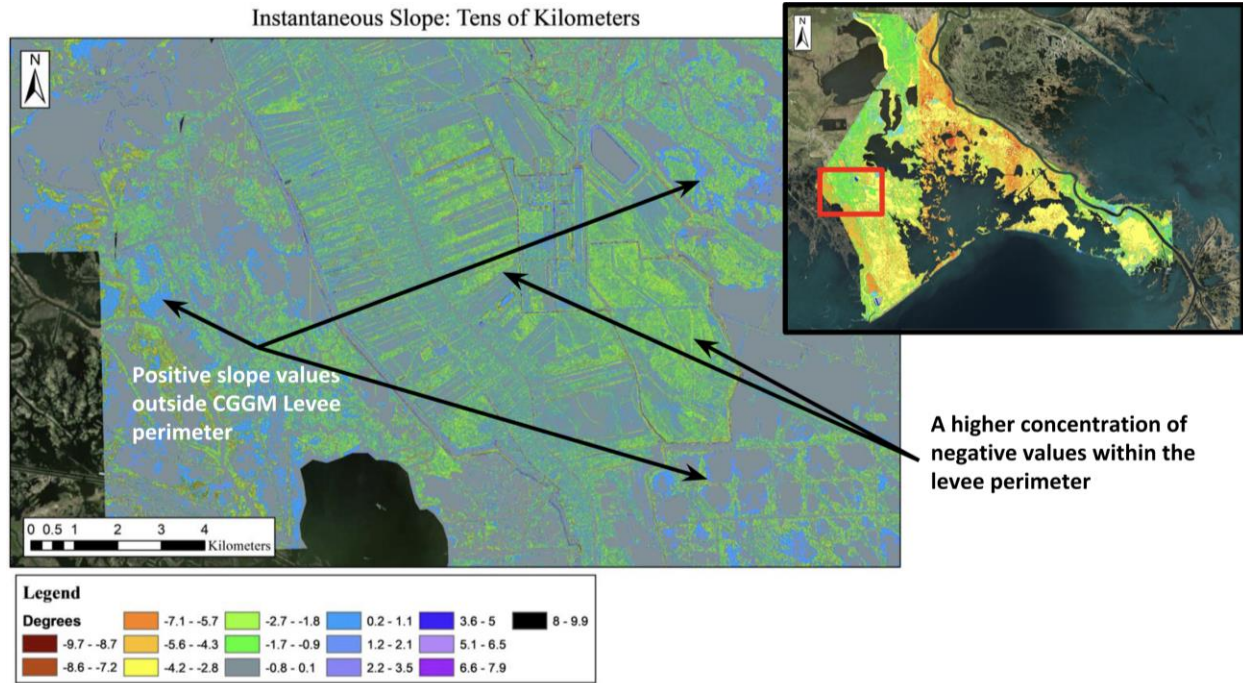


Figure 13: Instantaneous slope over the CGGM levee system showing a higher concentration of negative values within the levee perimeter and positive values outside; the blues along shorelines outside the levee perimeter indicate marsh edge loss. The negative values inside of the levee may indicate longer-term subsidence such as natural sediment compaction.

The importance of the instantaneous slope map is clear by viewing it in on spatial scales that range from 10^1 to 10^4 m. At the tens of kilometers scale, the CGGM Levee Complex models the effect of levees and leveed areas on subsidence rates. The Complex serves as a good model due to its central location in an area experiencing many of the known factors that contribute to land loss and subsidence in South Louisiana. On the basis of the instantaneous slope patterns within the CGGM Levee complex, (Figures 13) the expectation would be to see more negative values within the levees due to sediment starvation. In fact, Figure 13 shows a slightly higher concentration of negative values within the levee perimeter and positive values outside possibly indicate sediment starvation plays a role here.

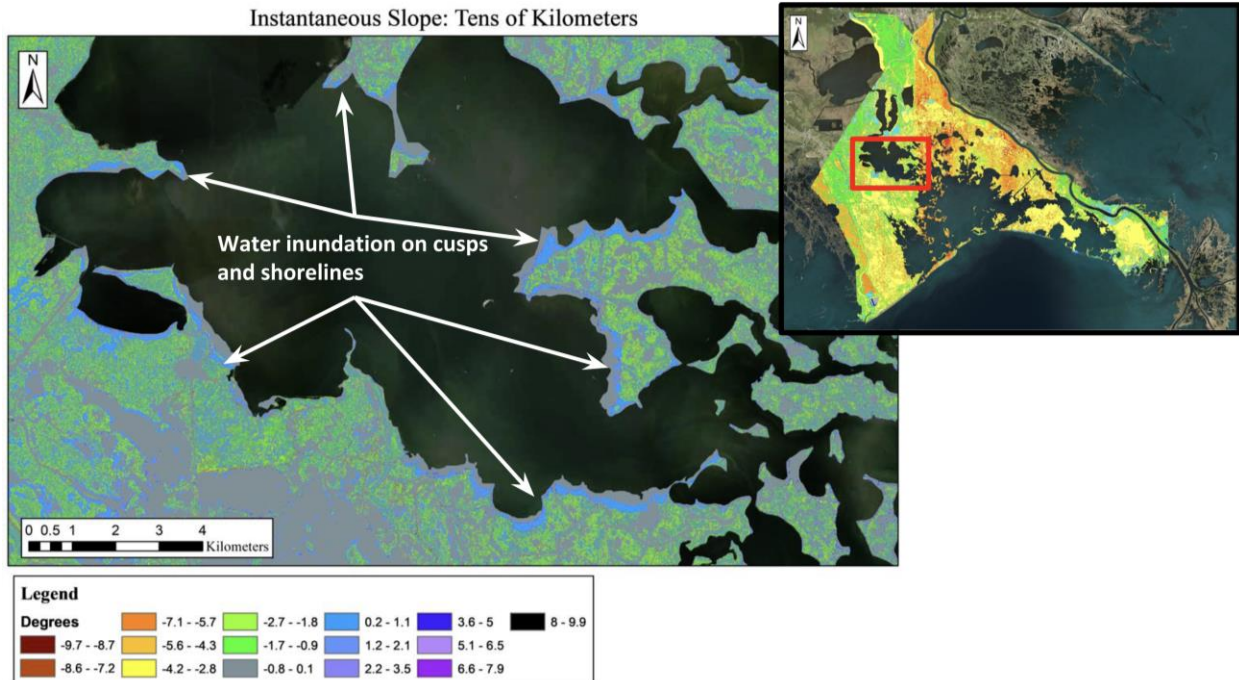


Figure 14: Slope values are distinctly positive on the shorelines of bays and cusps, specifically in the northwest section of Barataria Bay. Positive values range from 0.2 to 0.65 °. This indicates clearly that this is marsh edge loss; there was a relatively large elevation value in the earlier data that was converted to zero (or water level) in the newer data.

In Figure 14, bays within the Barataria Lidar data are studied in order to document trends on the tens of kilometers scale. Figures 14 show the slope values are distinctly positive on the shorelines of bays and cusps - specifically the northwest section of Barataria bay. Positive values range from 0.2 to 0.65 °.

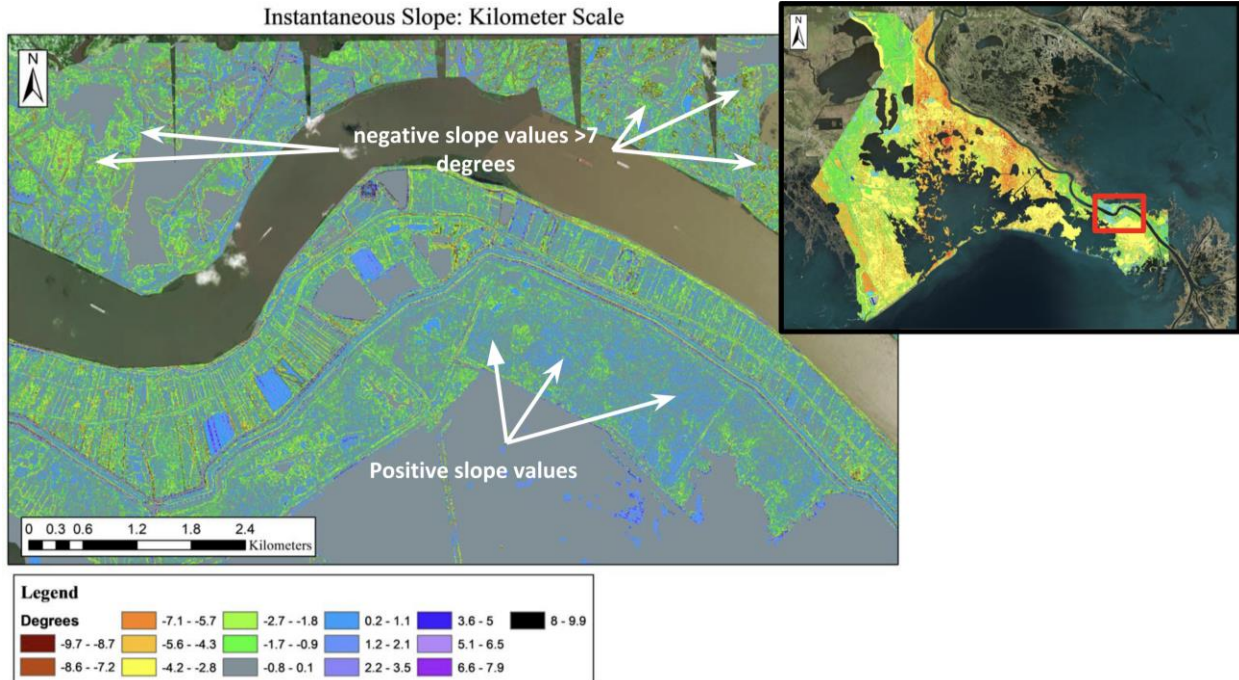


Figure 15: There is a higher concentration of negative slope values near Triumph, some exceeding 7° ; these values may indicate accretion or land building.

Instantaneous slope analysis seems to be the most useful on the spatial scale of kilometers. Figure 15 shows a higher concentration of negative slope values near Triumph. In the northwestern portion of the figure, there are clusters of highly negative values that exceed 7° . Like Figure 13, this site shows the effects of levees. Figure 16 shows in detail the effects of new construction, such as that completed in Port Fourchon within the data collection period.

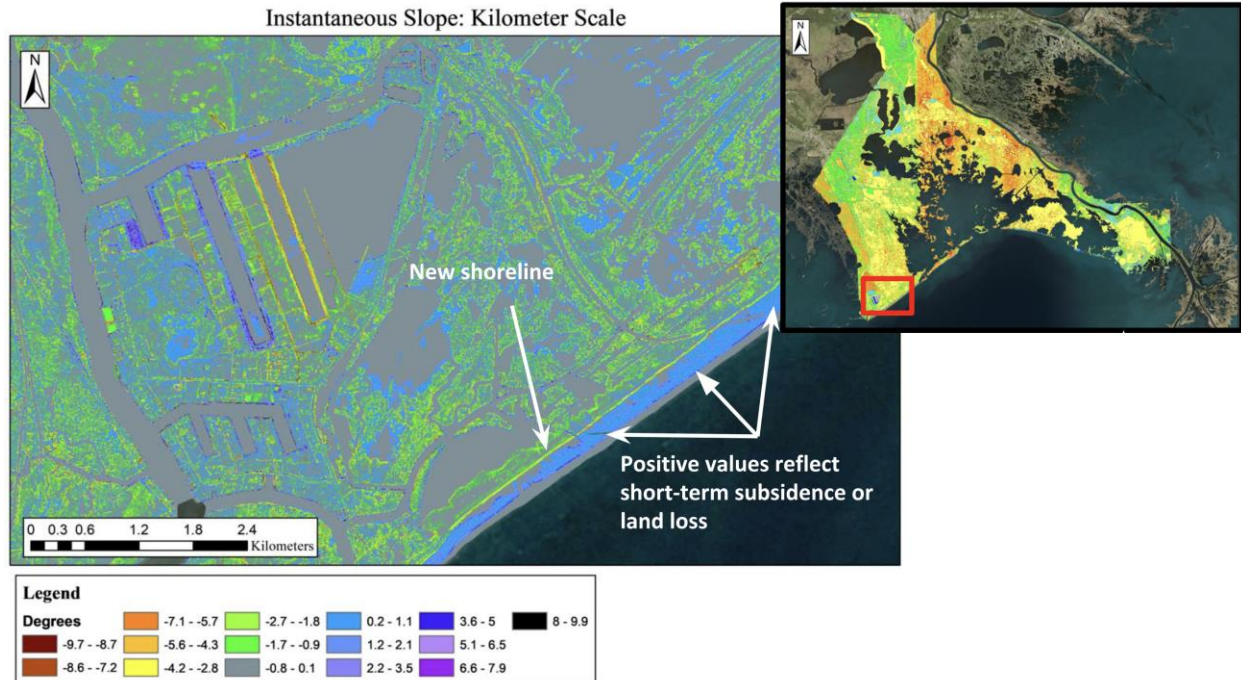


Figure 16: Negative slope values correspond with a low degree of variability in elevation in 2002 and a high degree of elevation variability in 2015. The areas around levees built between 2002 and 2015 or new construction in Port Fourchon exhibit this as new construction would increase the elevation variability.

B. Ancillary data with Raw data

1. Holocene Thickness

a. Raw data

The LOSCO Lidar data were differenced with the Depth to the Holocene-Pleistocene Boundary Map to yield the approximate thickness of the Holocene (Figure 10). The Holocene is thickest near the mouth of Mississippi, where the depth to the Holocene-Pleistocene boundary exceeds 90 m. Other locations of thick Holocene are found near Cutoff and central Terrebonne where depths to the boundary approach 70 m.

b. Processed data

In Figure 10, there is a clear, general thickening of the Holocene towards the modern Birdsfoot delta lobe. The borders of the Terrebonne Basin which are included in the study area also show slight thickening of the Holocene. It is possible that infilling of the latest Wisconsin incised valley of the Mississippi River with Holocene strata may account for this.

C. Ancillary Data with Difference Maps

To model the relationship between elevation change and factors that may contribute to elevation change in the Mississippi River Delta, key anthropogenic and non-anthropogenic features were spatially identified. These data include oil and gas wells, levees, salt domes and

coastal protection and restoration projects. In the dataset, there are 4300 oil and gas wells, which are located primarily over salt domes and within known oil fields. There are 5750 levees in the dataset, with many of the most important levees constructed in the 1980s. There are 1071 polygon features of restoration projects in this region, with key projects developed within the time period of this study. Finally, there are four major salt domes in this region, some of which are associated with the Marchand-Timbalier-Calliou salt-ridge complex, and the Golden Meadow Fault zone.

1. Oil and Gas Wells

a. Hundreds of Kilometers Scale

Oil and Gas Wells: Hundreds of Kilometers Scale

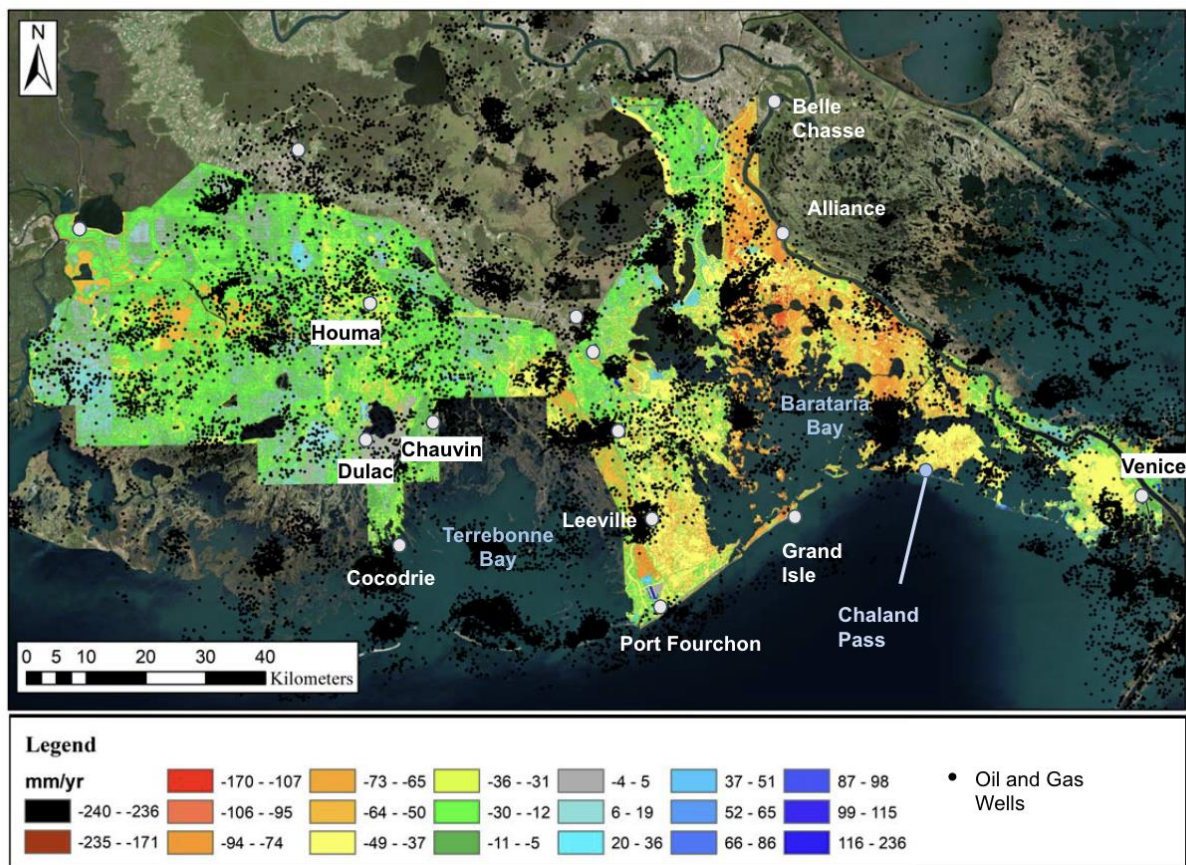


Figure 17: This figure shows the locations of all known oil and gas wells in SE Louisiana; Here, the subsidence map is overlain by the oil and gas well shapefile acquired from the Louisiana Department of Natural Resources (LDNR) SONRIS database.

In Figure 17 the Lidar difference map is overlain by the LDNR SONRIS shapefile of oil and gas well sites. As expected, clusters of well sites are concentrated on the surface above known salt domes. There is no clear trend of increased concentration of extraction wells and increased change in land elevation rate at this scale.

b. Tens of Kilometers Scale

For the tens of kilometers scale, the areas approximately overlaying the Clovelly and Bully Camp salt domes model the potential effects that oil and gas production may have on subsidence. At Bully Camp and Clovelly, the wells are clustered over the approximate location of the salt dome.

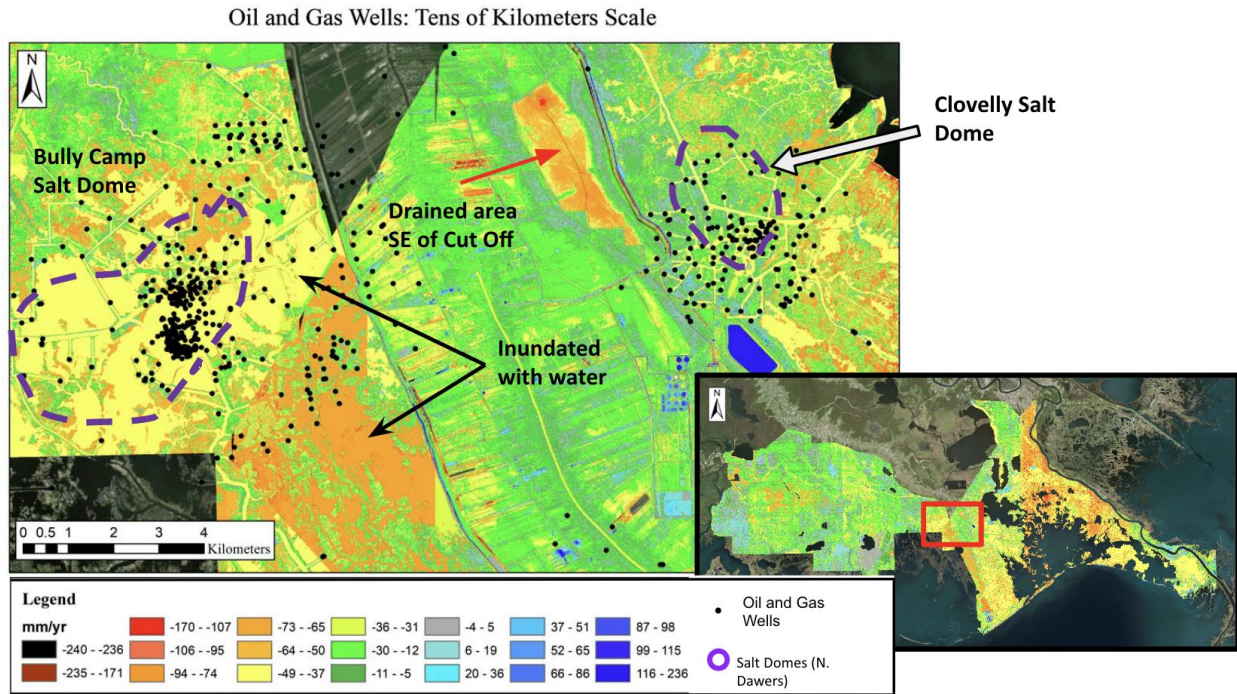


Figure 18: Wells are clustered over the approximate location of the Bully Camp and Clovelly salt domes. The salt dome locations are projected to their land surface locations from their known intersections with the Pleistocene surface.

Figure 18 shows the concentration of well sites over the Clovelly salt dome on the east side (also see Figure 35) and Bully Camp on the west side (also see Figure 33). Subsidence over the Clovelly salt dome is as much as -110 mm/yr in some very localized areas. The land surface above the Bully Camp salt dome has subsidence rates as high as -90 mm/yr, observed most often within marsh edge environments.

c. Kilometer Scale

For the kilometer scale analysis of subsurface fluid production, elevation changes were observed in the leveed area west of Chauvin (Figure 19) and the Venice salt dome (Figure 20).

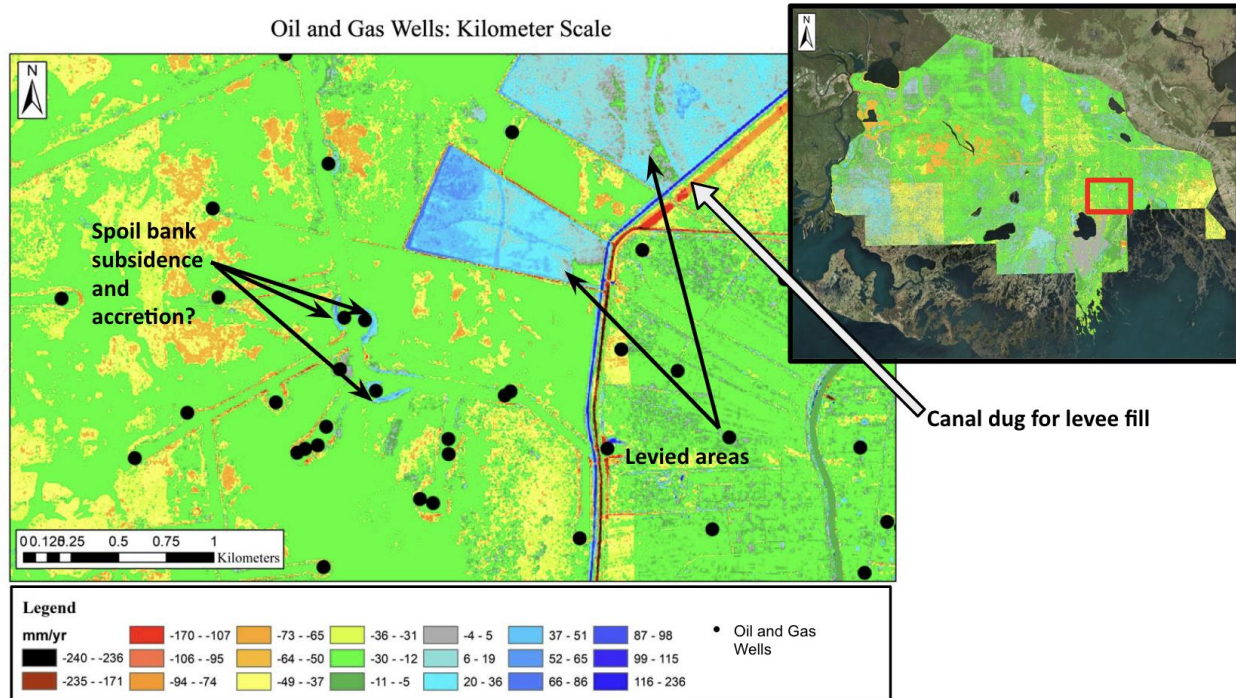


Figure 19: Just west of Chauvin, LA, oil and gas wells are observed outside of a levee system; some spoil banks show accretion only meters from a well site, whereas others show significant subsidence within the same spatial parameters. Wells in the center showing land elevation gain may actually be berms and equipment for the wells installed within the time between the different Lidar datasets.

The leveed area west of Chauvin was chosen because there are fewer concerns about the role of salt as a control of subsidence in this area. In addition, the area is primarily marshland so positive or negative land elevation changes were clear and immediate.

The Venice salt dome offers higher variance in land elevation change rates as its location near the Birdsfoot makes it part of a highly dynamic environment. Observing the pattern of accumulation and subsidence in the land surface over the Venice salt dome can indicate if subsidence due to subsurface fluid extraction is capable of out-pacing accretion near the river mouth.

Wells focused in the center of Figure 19 show a high variability in land surface vertical motion. Some areas are accreting at rates of as much as 56 mm/yr only meters from a well site, whereas others show subsidence of as much as -106 mm/yr within the same spatial parameters.

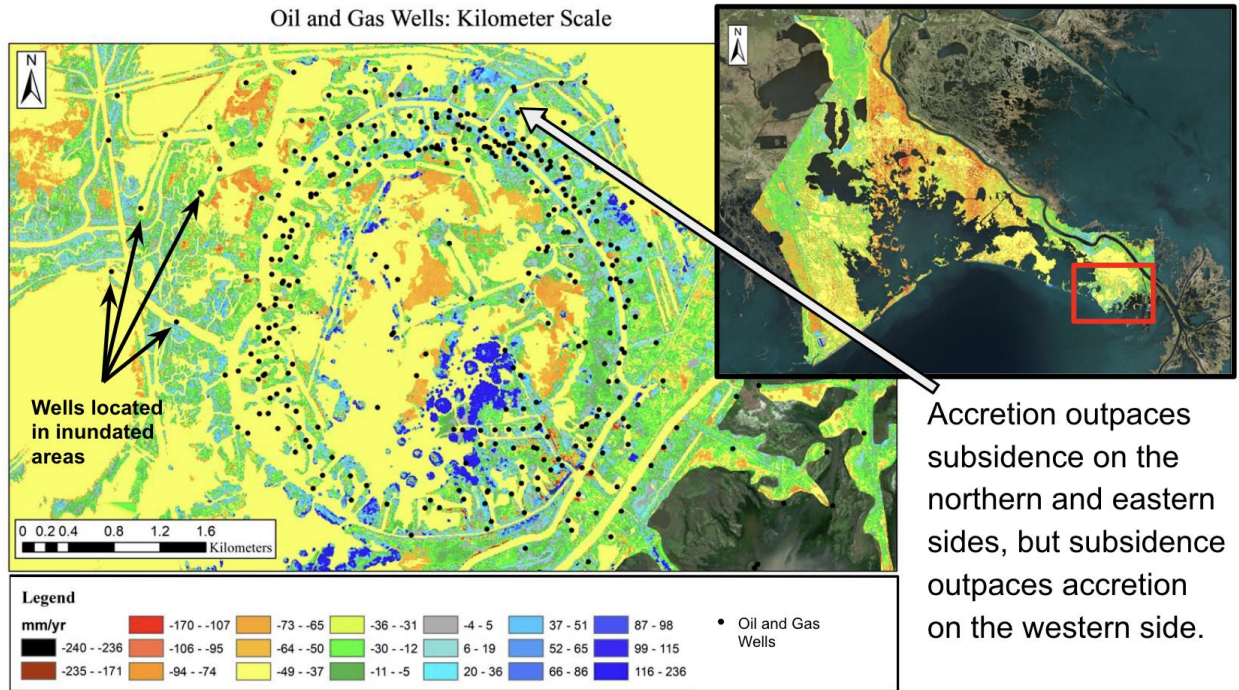


Figure 20: The Venice salt dome shows a higher variance in land elevation change rates as its location near the Birdsfoot delta makes it part of a highly dynamic environment. Many oil and gas wells are situated in what is now water, particularly on the western side of the dome’s surficial expression. On the northeastern side, however, many wells appear in areas showing high accretion rates (up to 51 mm/yr).

Figure 20 shows the well sites surrounding the Venice salt dome. Many oil and gas wells are situated in what is now water, particularly on the western side of the dome’s surficial expression. This makes it impossible to determine subsidence rates in their immediate vicinity. On the northeastern side, however, many wells appear in areas showing high accretion rates- some as much as 51 mm/yr. Figure 21 varies greatly from the dynamic system near the mouth of the river. The Leeville salt dome also has a large number of oil and gas wells producing over and around it, however there is not as much variation in elevation rates as there are at the Venice salt dome site.

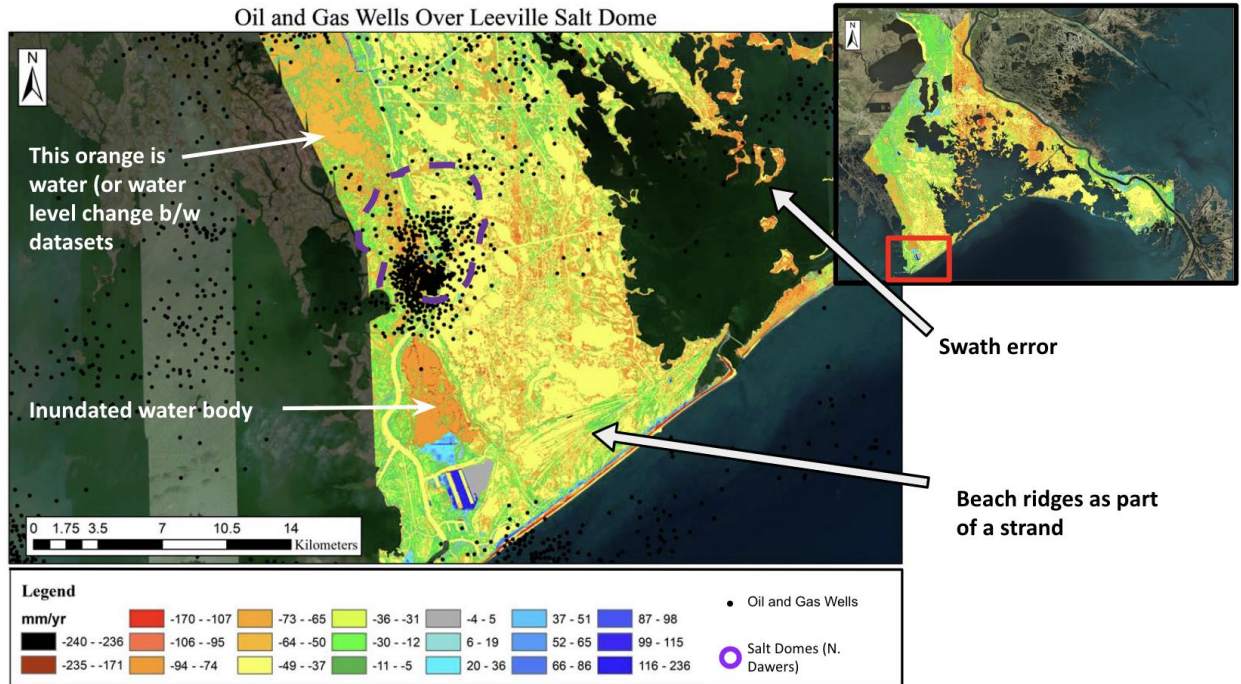


Figure 21: Observing the Leeville Salt Dome area, it's impossible to determine if there is a correlation with land elevation change rates and salt motion or subsurface fluid withdrawal.

2. Levees

a. Hundreds of Kilometers Scale

In Figure 22 the Lidar difference map is overlain by a shapefile of the levee system. Within the confines of the levees, the stretch from Cutoff to Golden Meadow is clearly defined by slower rates of subsidence than the surrounding areas.

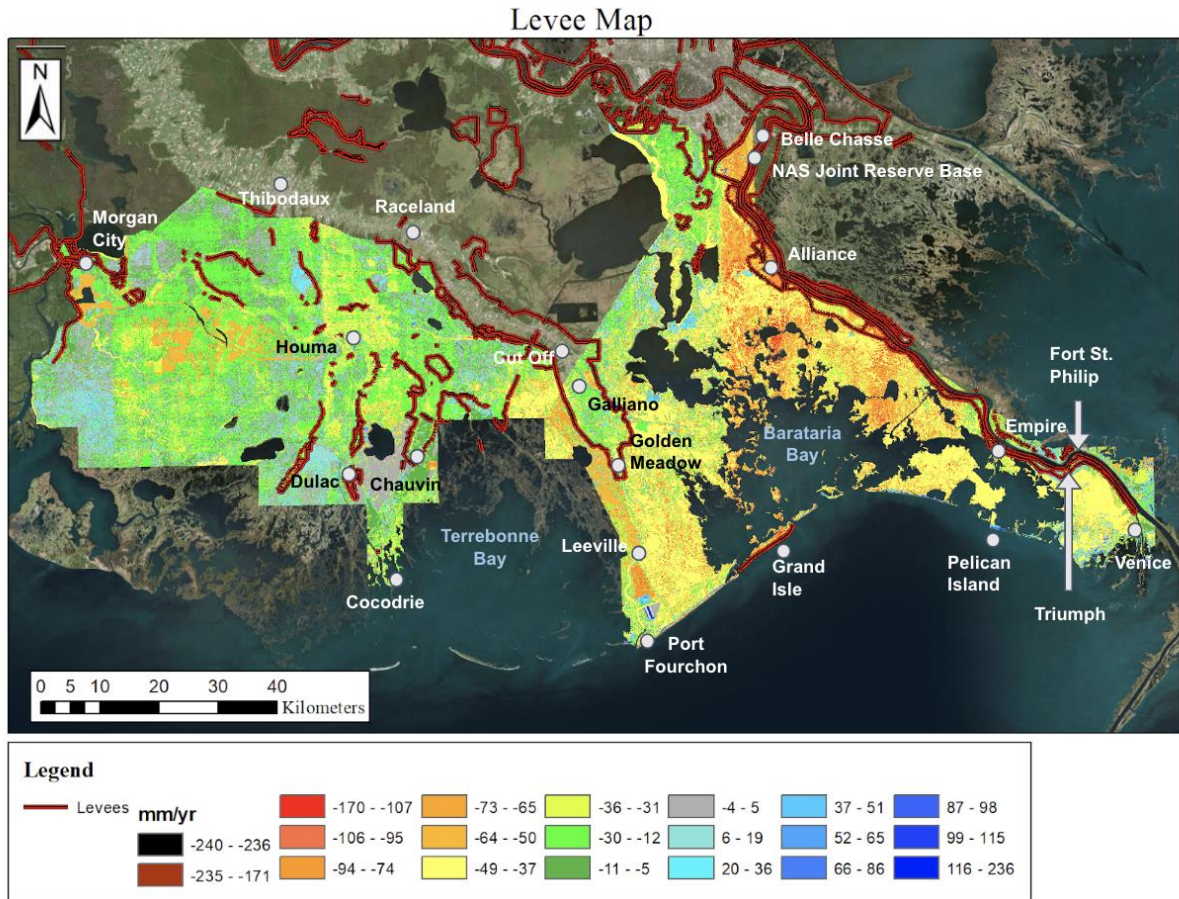


Figure 22: This figure shows the locations of all known levees in SE Louisiana; Here, the subsidence map is overlain by the levee shapefile acquired from the Louisiana Department of Natural Resources (LDNR) SONRIS database. Within the confines of the levees, the stretch from Cutoff to Golden Meadow is clearly defined by slower rates of subsidence than the surrounding areas.

b. Tens of Kilometers Scale

The impact levees can have on subsidence rates at the tens of kilometers scale is clear, especially within the CGGM Levee System. This is a good model for how a complete levee system, geographically positioned within inundated marsh land, can impact subsidence rates. At the tens of kilometers scale, areas within levees subside at lower rates than areas outside the levee system. Rates within levee systems are generally -30 to -5 mm/yr vertical loss whereas surrounding areas are subsiding at rates as high as -70 mm/yr (Figure 23). The effect of the levee is not as evident on the eastern side, near Golden Meadow.

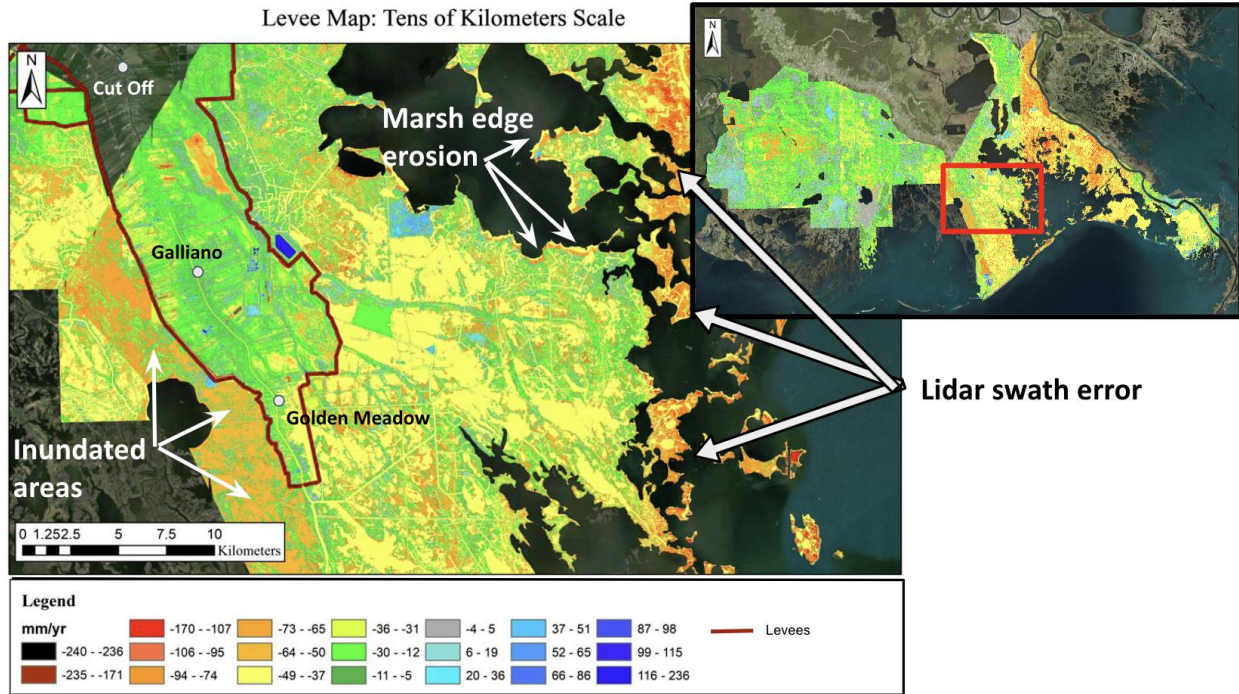


Figure 23: The CGGM Levee System is a good model for how a complete levee system, geographically positioned within inundated marshland, can impact subsidence rates. At the tens of kilometers scale, areas within levees subside at lower rates than areas outside the levee system. Rates within levee systems are generally -30 to -5 mm/yr vertical loss whereas surrounding areas are subsiding at rates as high as -70 mm/yr.

c. Kilometer Scale

The Leonard Farm Site in Figure 24 is located in the leveed area just west of Chauvin near Lake Boudreaux. The smaller leveed areas were observed for the role levees play on the kilometer scale. Spatial changes in subsidence rate can vary substantially by the meter in this area, making it ideal for studying levee effects on subsidence at the kilometer scale.

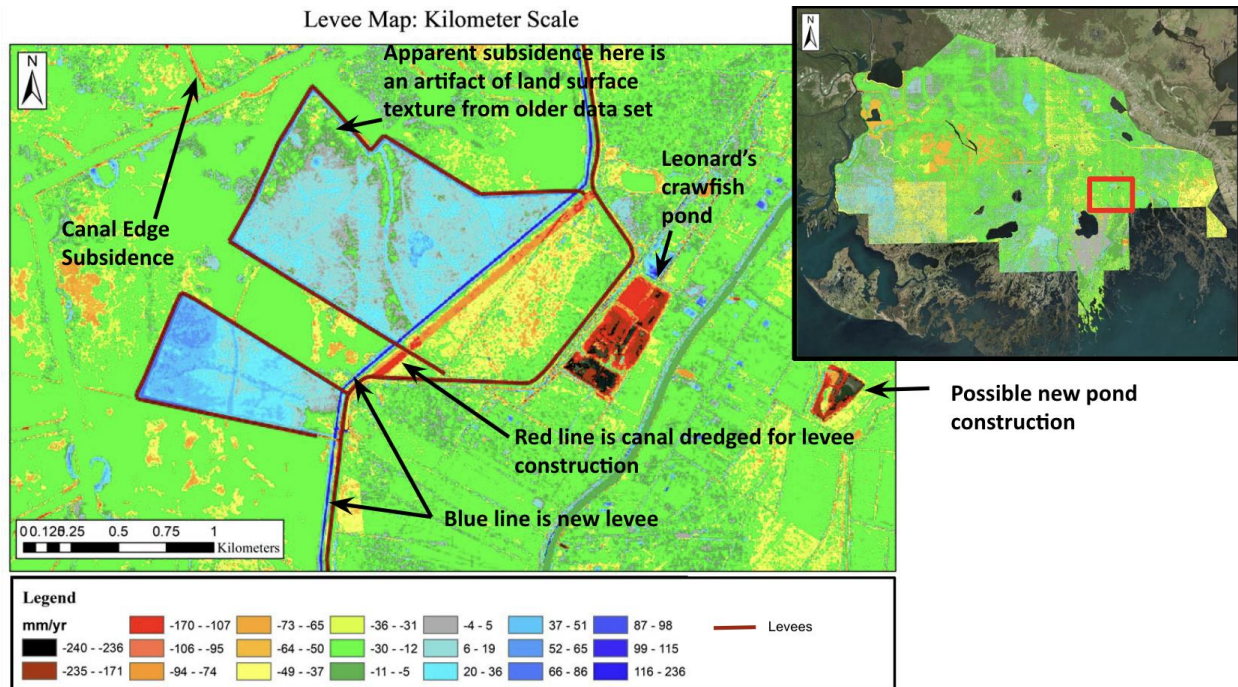


Figure 24: This site is located in the leveed area just west of Chauvin near Lake Boudreaux. The levees clearly infilled with blue were likely constructed in 2011 (between the 2002 and 2015 collection dates of the differenced Lidar datasets). The apparent accretion inside the levee is actually caused by a water level in the new data that was higher in elevation than the land surface was in the older (2002) data. It seems to have texture because of the marsh that was there in the earlier data.

The figure shows the basins confined by levees appear to be accreting as much as 65 mm/yr whereas the surrounding area shows general subsidence of approximately 30 to 65 mm/yr. The western levees were likely constructed in 2011- between the 2002 and 2015 collection dates of the differenced Lidar datasets. Just north of Dulac, the West Lake Boudreaux Shoreline Protection Project site displays the effective use of levee systems (Figure 25). Marsh edge erosion has eliminated much of the land east of the levee. However, on the protected side of the levee, land is preserved with slightly higher subsidence rates than the land in the western portion of the figure.

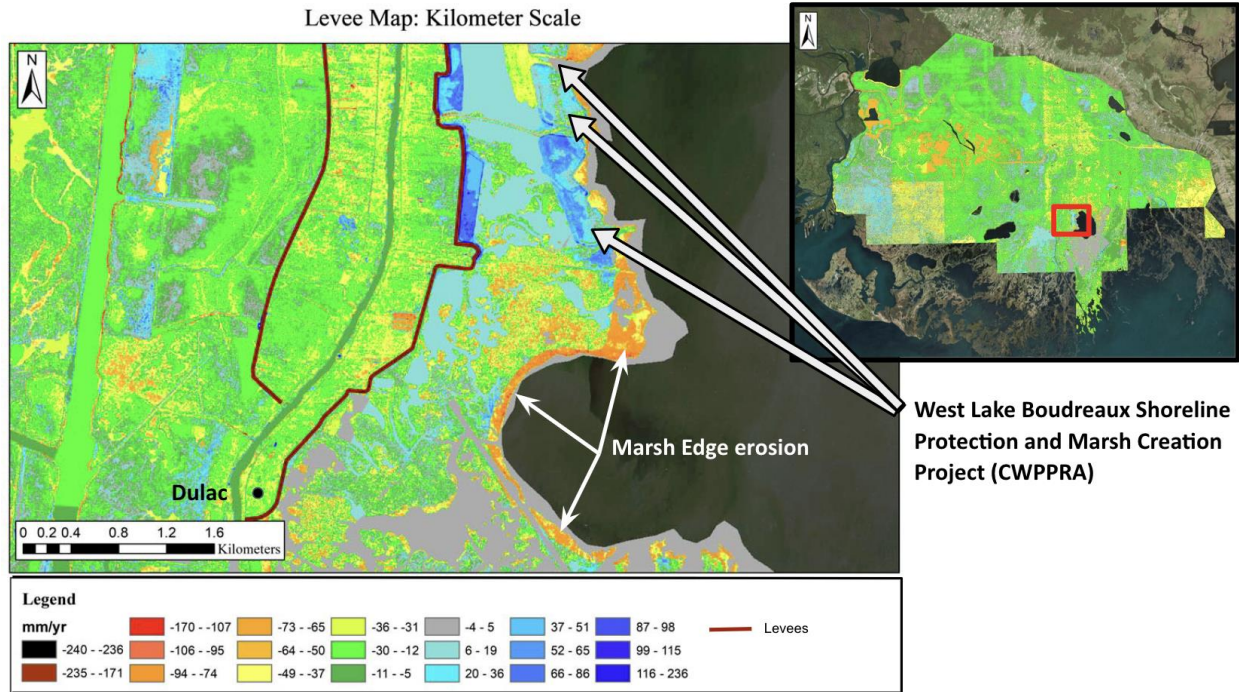


Figure 25: The site near Dulac provides examples of effective levee systems as well as marsh edge erosion. The land is gone east of the levee, but west of it, it is preserved with slightly higher subsidence rates than the land in the western portion of the figure.

Just south of Avondale, Figure 26 shows the increased subsidence within the leveed area versus the area outside of it. Much of the area outside the levee has subsidence near zero or is accreting, but the subsidence rates within the levee may exceed -170 mm/yr. Just east of Montegut, there is apparent accretion occurring just south of the more western levee (Figure 27). This may be due to sediment deposition or relative water level being higher in newer data due to the marshes outside of levee system keeping pace with RSLR.

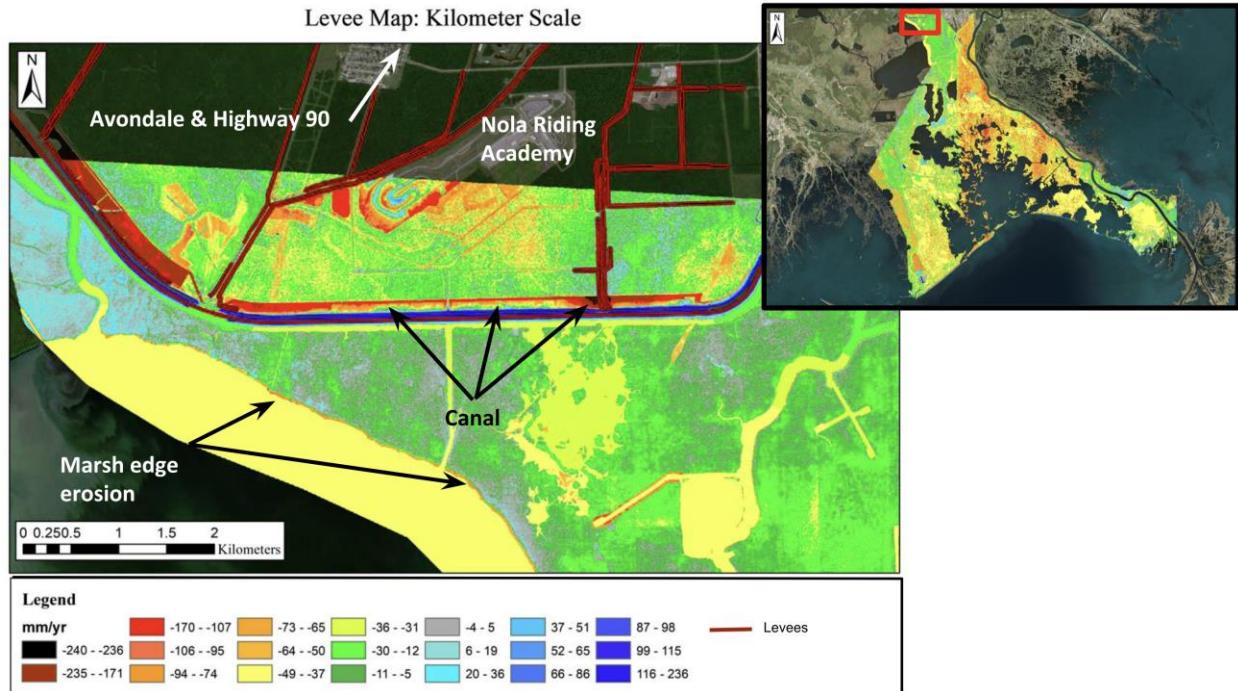


Figure 26: Just south of Avondale, increased subsidence has occurred within the leveed area versus the area outside of it. Much of the area outside the levee has subsidence near zero or accreting, but the subsidence rates within the levee may exceed -170 mm/yr.

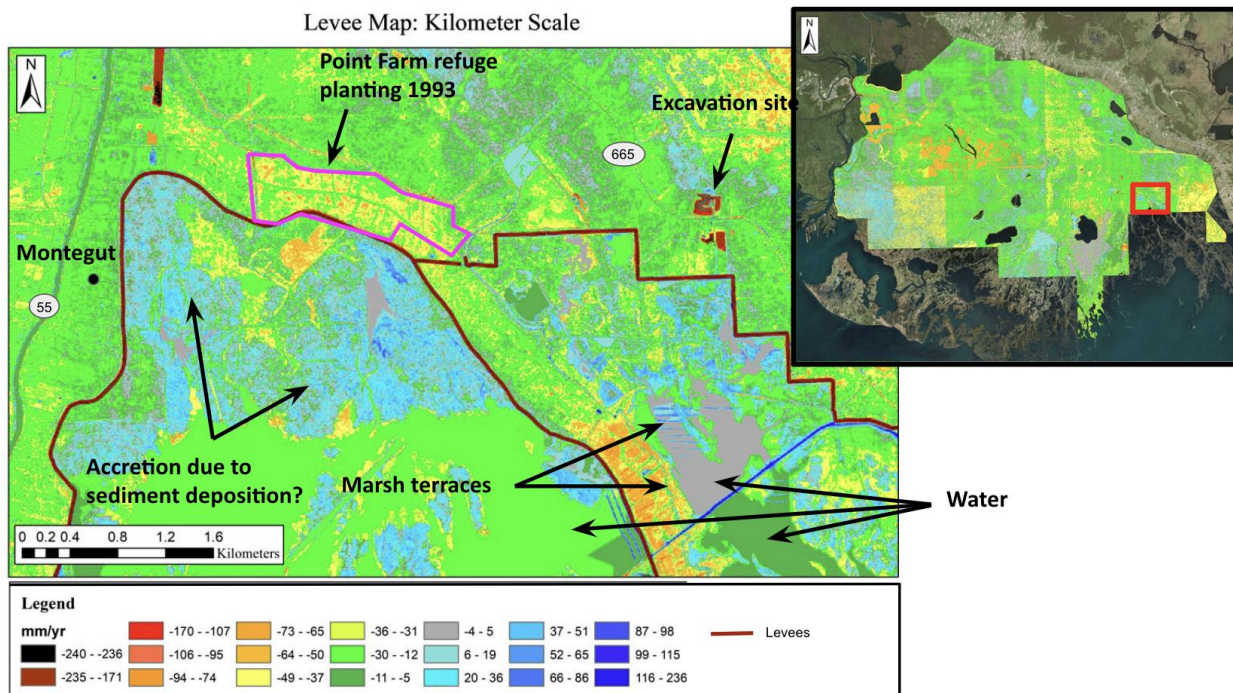


Figure 27: Near Montegut, there is apparent accretion occurring just south of the more western levee; this may be due to sediment deposition or a higher relative water level in newer data due to the marshes outside of levee system keeping pace with RSLR. Additionally, the Point Farm refuge planting included 75 acres of bitter pecan, cow oak, nuttall oak and water oak, planted in 1993. The project was completed by CPRA and included a total of 363 trees.

3. Coastal Protection Project Sites

a. Hundreds of Kilometers Scale

At this scale, it is clear that there is a significant amount of protection efforts across southeast Louisiana (Figure 28). All completed projects show a positive vertical change in land surface on the scale of tens of mm/yr.

Coastal Restoration Project Sites: Hundreds of Kilometers

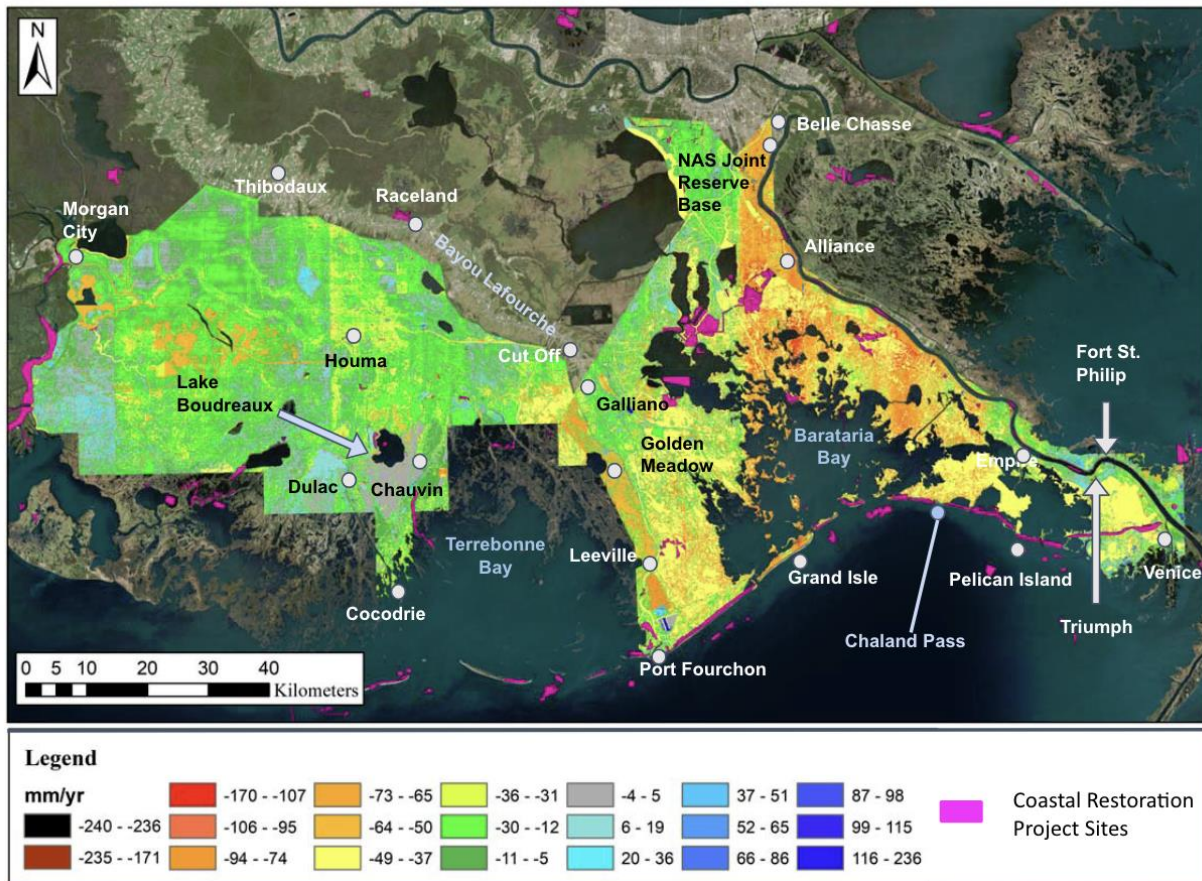


Figure 28: This figure shows the locations of all known Coastal Restoration Projects in southeast Louisiana; Here, the subsidence map is overlain by the Coastal Restoration Project shapefile acquired from the Louisiana Department of Natural Resources (LDNR) SONRIS database.

b. Tens of Kilometers Scale

The Little Lake Shoreline Protection marsh creation project, shown in Figures 29 and 29b, is a good example of the effect of projects on the tens of kilometers scale because it is the largest project completed within the study area and it was constructed within the period of data collection.

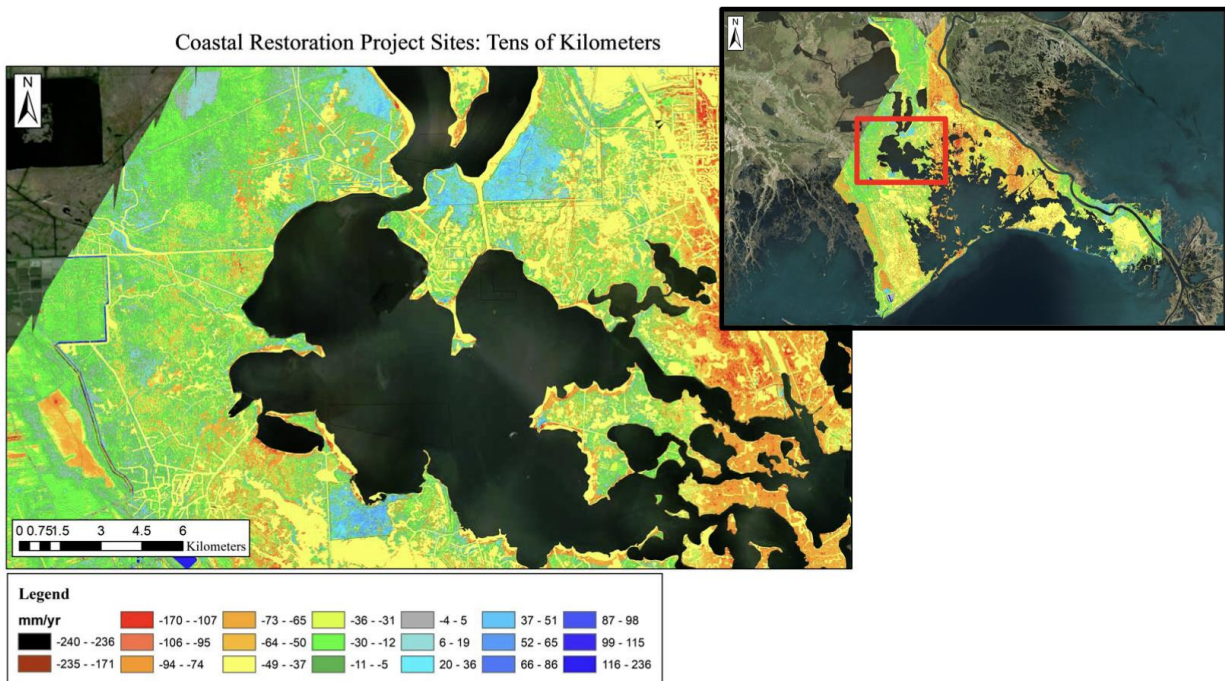


Figure 29: The Little Lake Shoreline Protection marsh creation project, is a good example of the effect of projects on the tens of kilometers scale because it is the largest project completed within the study area and it was constructed within the period of data collection. There is a notable difference of positive vertical change (6 to 65 mm/yr) within the project area in comparison to surrounding areas (-73 to -12 mm/yr).

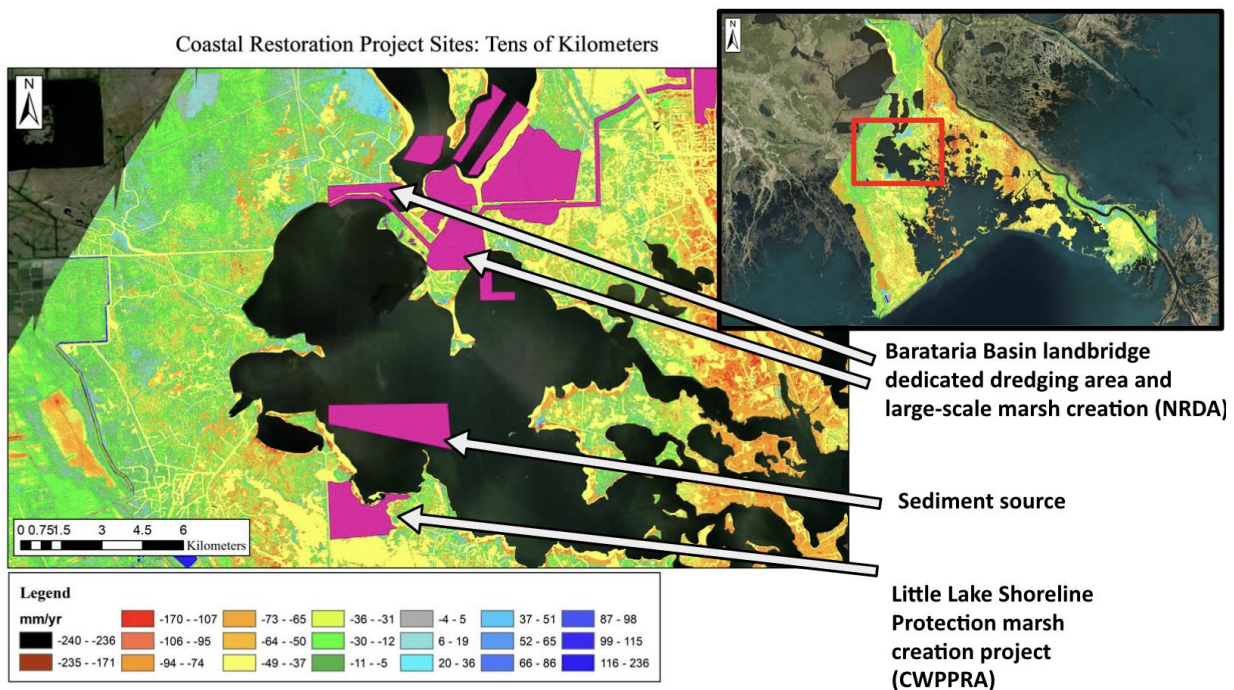


Figure 29b: The Little Lake Shoreline Protection Project, completed by the Coastal Wetlands Planning, Protection and Restoration Act (CWPPRA), had a construction date of 3/1/2007, putting it in between the collection dates of the differenced Lidar data maps (2002/3-2015); The project focused on marsh nourishment, adding 2,162,906 m² of dredged material to create 0.76 m of elevation in 3.84 km² of marshland (based on NAVD 88 elevation).

There is a notable difference of positive vertical change (6 to 65 mm/yr) within the project area in comparison to surrounding areas (-73 to -12 mm/yr). The Little Lake Shoreline Protection Project, completed by the Coastal Wetlands Planning, Protection and Restoration Act (CWPPRA), had a construction date of 3/1/2007, putting it in between the collection dates of the differenced Lidar data maps (2002/3-2015). The project focused on marsh nourishment, adding 2,162,906 m² (2,828,974 cubic yards) of dredged material to create 0.76 m (2.5 ft) of elevation in 3.84 km² (950 acres) of marshland (based on NAVD 88 elevation).

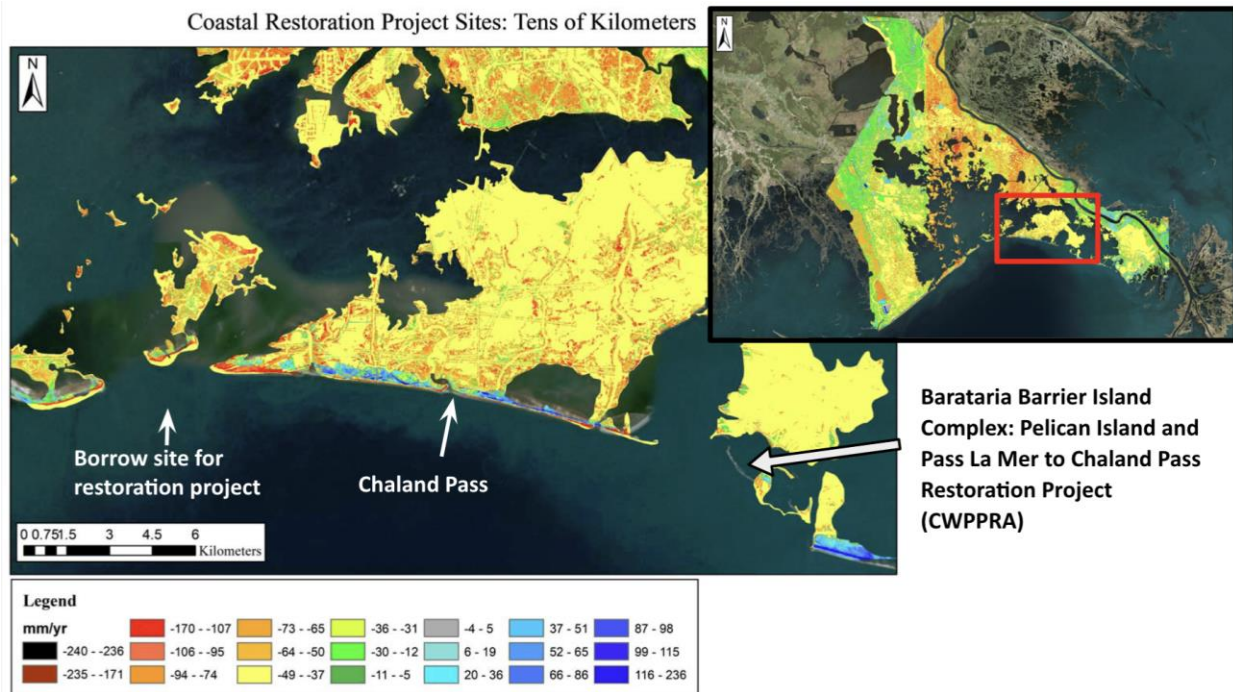


Figure 30: CWPPRA’s Barataria Barrier Island Complex: Pelican Island and Pass La Mer to Chaland Pass Restoration Project is shown with positive vertical changes concentrated in the overwash areas. This site is significant to our study due to drastic changes in elevation it created over tens of kilometers within the study period. The positive trends exceed 100 mm/yr in some areas.

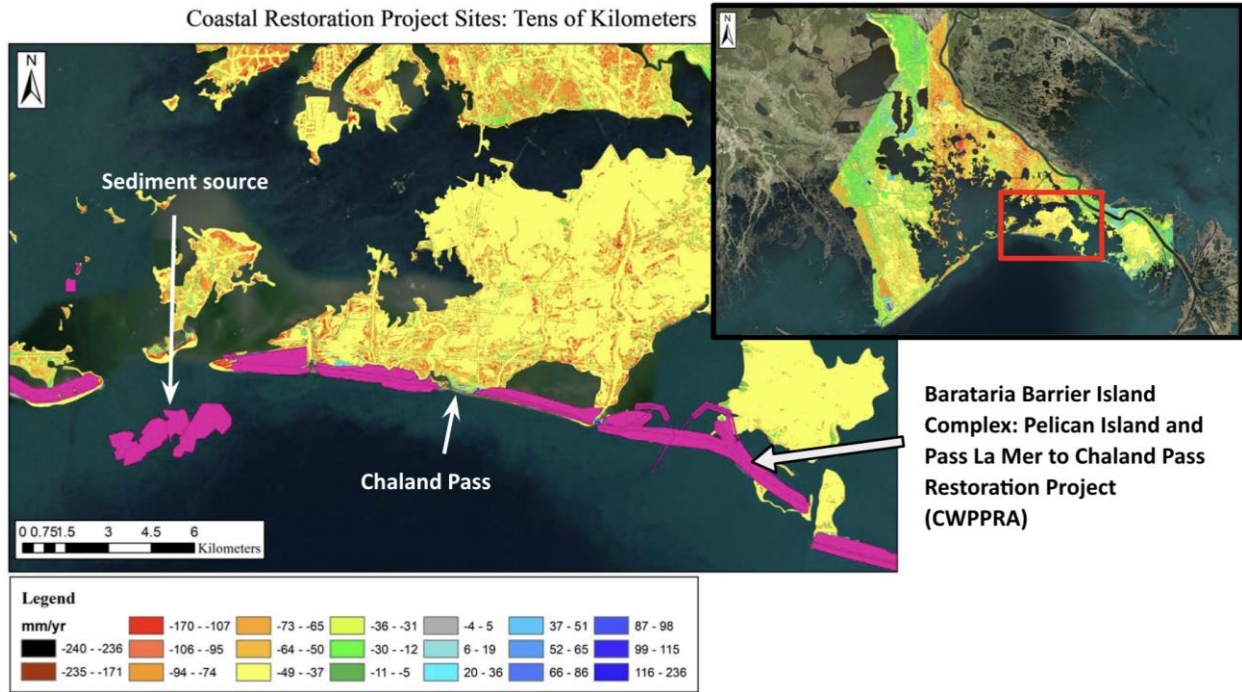


Figure 30b: The Barataria Barrier Island Complex: Pelican Island and Pass La Mer to Chaland Pass Restoration Project is a beach fill project with a construction date of 11/28/2012.

CWPPRA’s Barataria Barrier Island Complex: Pelican Island and Pass La Mer to Chaland Pass Restoration Project is shown in Figure 30 and 30b with positive vertical changes concentrated in the overwash platforms. This site is significant to our study due to drastic changes in elevation it created over tens of kilometers within the study period. The positive trends exceed 100 mm/yr in some areas. This is a beach fill project with a construction date of 11/28/2012.

c. Kilometer Scale

Figure 31 and 31b show the West Lake Boudreaux Shoreline Protection and Marsh Creation Project (CWPPRA), which is a dredge fill project completed on 10/31/2009. Like the others, this project was completed within the data collection period for this study. However, it was a slightly smaller endeavor, creating less than 300 acres of marsh. Throughout the project site there are positive vertical change values. In some areas, these exceed 50 mm/yr.

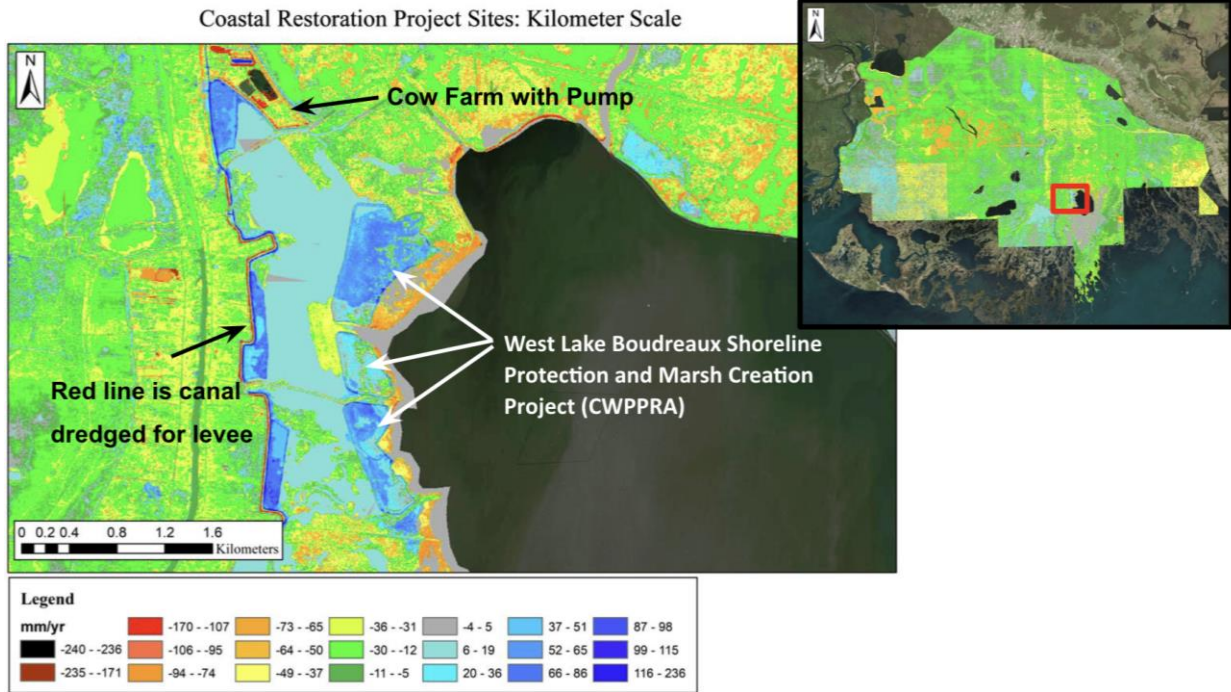


Figure 31: The West Lake Boudreaux Shoreline Protection and Marsh Creation Project (CWPPRA) is a dredge fill project completed on 10/31/2009. Like the others, this project was completed within the data collection period for this study. However, it was a slightly smaller endeavor, creating less than 300 acres of marsh.

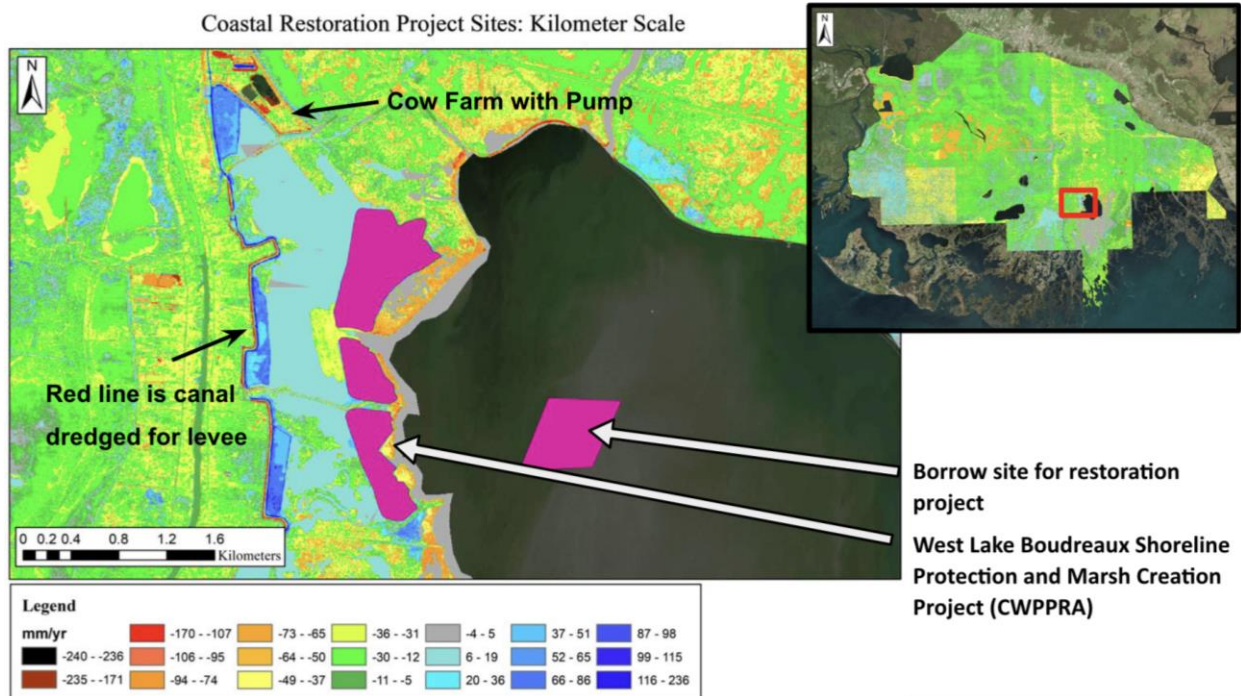


Figure 31b: Throughout the West Lake Boudreaux Shoreline Protection and Marsh Creation Project site there are positive vertical change values. In some areas, these exceed 50 mm/yr.

It is important to note that many of these projects were started within the 2002/3-2015-time period between the collections of the differenced datasets. Therefore, the full impact of these projects cannot be represented within this study.

4. Salt Domes

a. Hundreds of Kilometers Scale

At the hundreds of kilometers scale, there is no obvious visual correlation between salt dome location and surface elevation change within the time scale of our study (Figure 32).

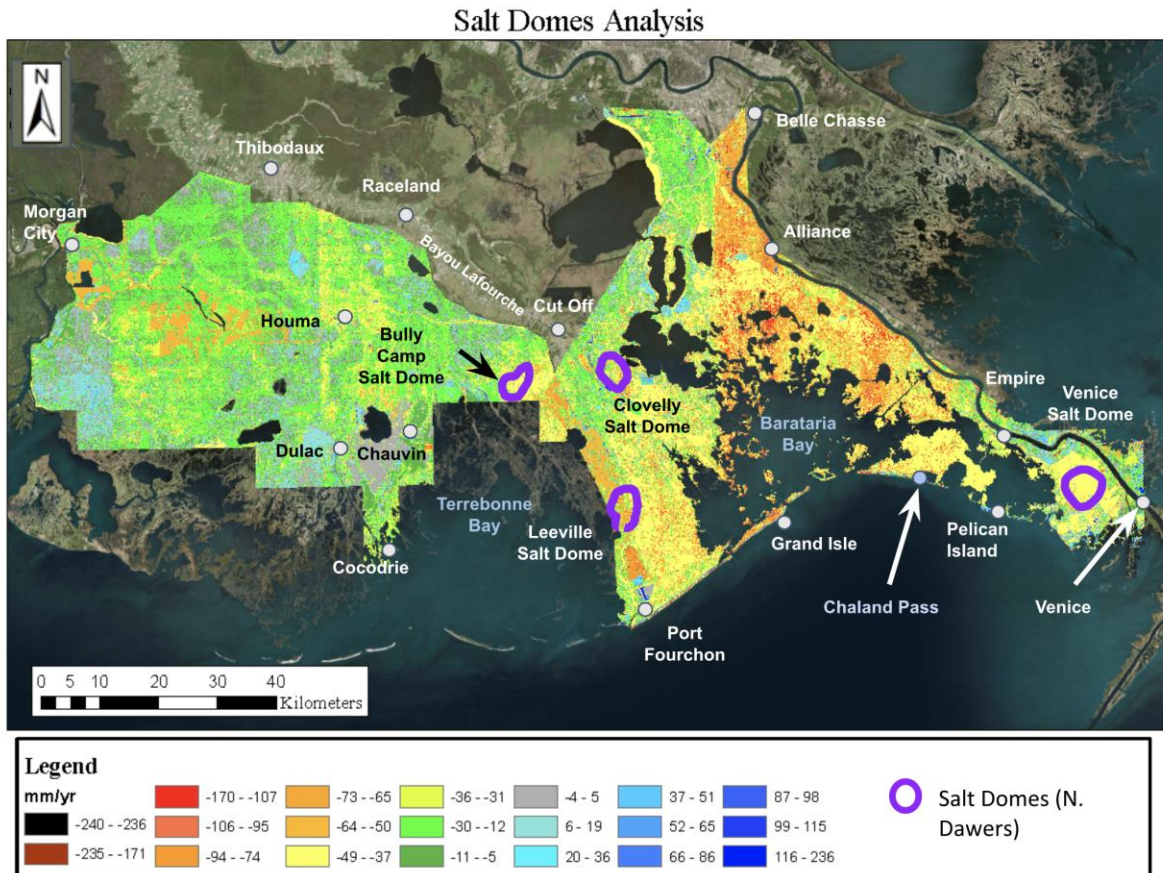


Figure 32: This figure shows the locations of a few notable salt domes in southeast Louisiana; the subsidence map is overlain by surficial projections of the salt dome’s intersections with the Holocene-Pleistocene surface. These data were gathered from Nancye Dawers (pers. comm.) and Chris McLindon (pers. comm.).

b. Tens of Kilometers Scale: Bully Camp and Leeville

The Bully Camp salt dome provides an example of the impacts salt domes may have on surficial subsidence rates at the tens of kilometers scale because it is the largest salt dome within the study area (Figure 33). The Bully Camp salt dome is largely overlain by water (Lake Bully Camp) so an analysis was conducted with the Lidar data of remaining land over the dome. The

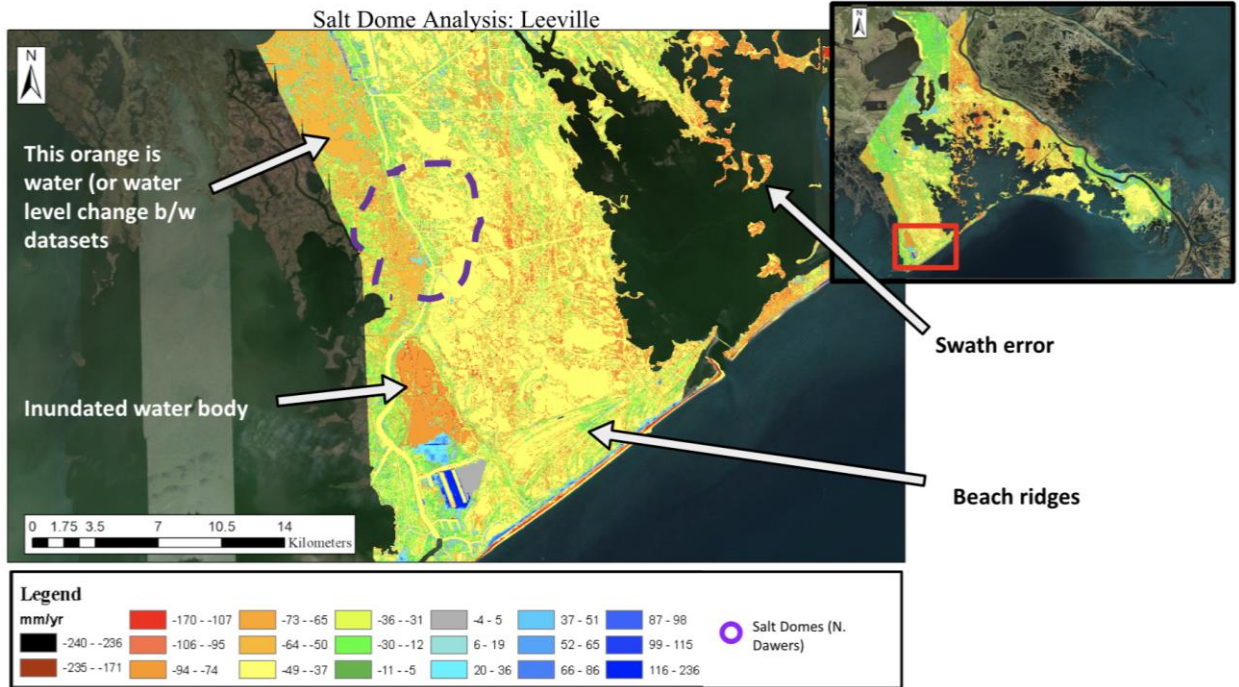


Figure 34: The surface expression of the Leeville salt dome is notable due to a greater degree of variance in vertical change values compared to surrounding areas. Although larger subsidence values appear directly above the predicted location of the dome, there is also measurable accretion.

c. Kilometer Scale: Clovelly and Venice

The Clovelly salt dome is smaller than the Bully Camp dome and impacts the land surface on a smaller scale, which makes it a good model for kilometer-scale study. The Clovelly salt dome is overlain by a land surface with a generalized increase in subsidence rates from the surrounding area (Figure 35). The difference may be anywhere from 20-50 mm/yr higher than nearby areas. There is also a concentrated number of canals directly over the estimated location of the salt dome.

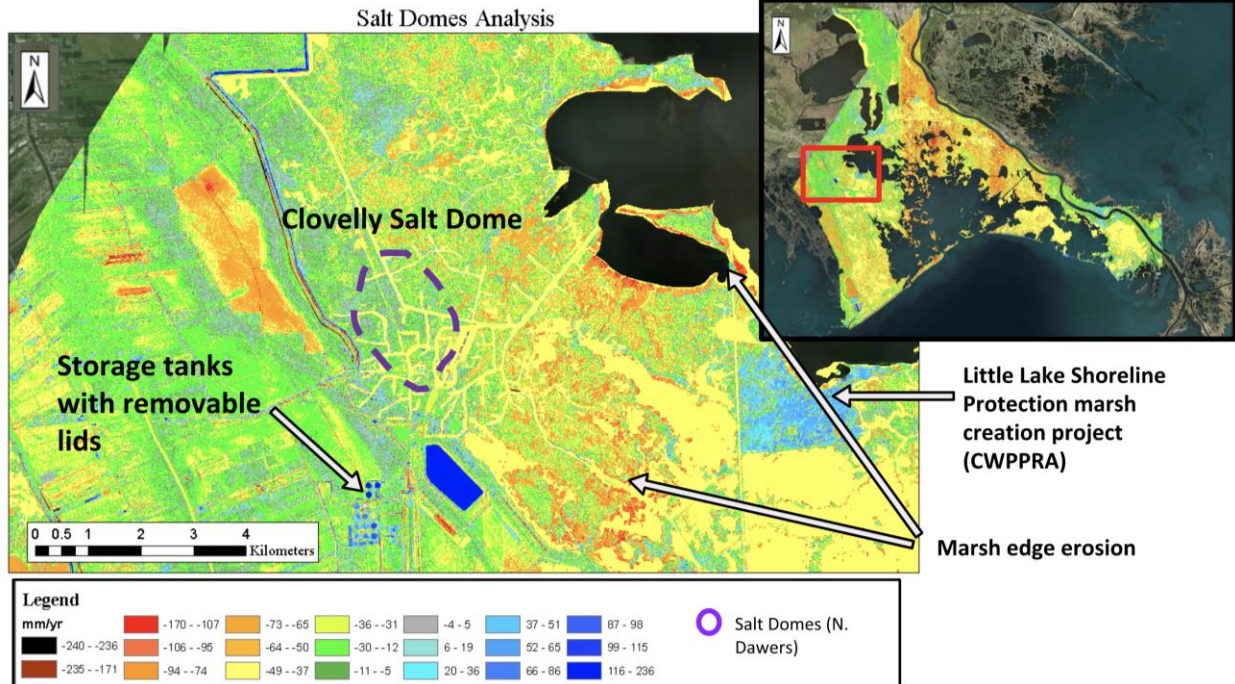


Figure 35: There is a generalized increase (from -20 to -50 mm/yr greater than surrounding areas) in subsidence rates over the surficial projection of the Clovelly salt dome. It is also important to note that there is a concentrated number of canals directly over the estimated location of the salt dome.

Like Clovelly, the Venice salt dome has a higher concentration of variable subsidence rates, which makes it a more effective study for kilometer-scale observations. Figure 36 shows the approximate location of the Venice salt dome as well as a clear surface expression in the differenced Lidar data. The apparent offset of the dome top location is due to the depth at which the dome was observed at the Holocene-Pleistocene boundary rather than the land surface. Some greater subsidence can be seen inside of the circular surface expression of the dome. Here, rates are as high as -95 mm/yr. However, positive elevation change values are found on the northeast side. Again, this is a highly active oil and gas production area as noted in Figure 20.

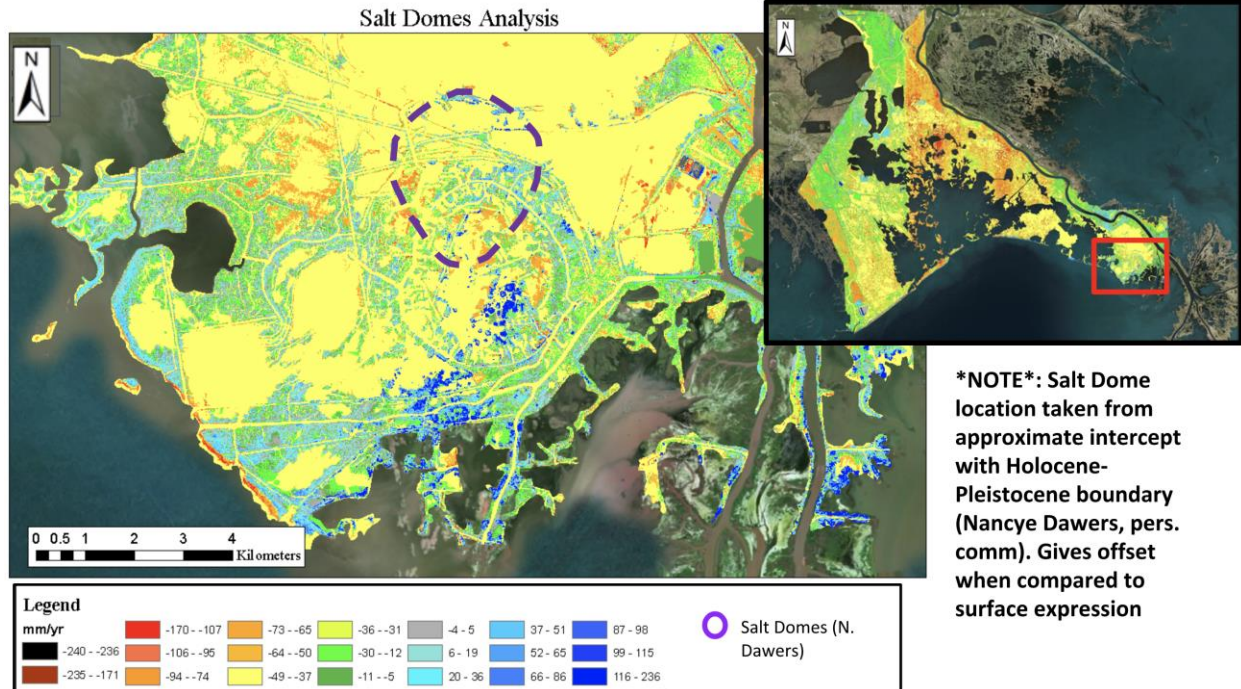


Figure 36: The apparent offset of the dome top location is due to the depth at which the dome was observed at the Holocene-Pleistocene boundary rather than the land surface. Like Clovelly, the Venice salt dome has a higher concentration of variable subsidence rates, which makes it a more effective study for kilometer-scale observations. Some higher subsidence are present inside of the circular surface expression of the dome (rates ~ -95 mm/yr), however, positive elevation change values are found on the northeastern side. This is a highly active oil and gas production area as noted in Figure 20. The cause of the strongly positive values in the center and more southwestern portions of the dome expression cannot be clearly accounted for.

IV. Discussion

A. SUBSIDENCE

There are questions and controversies regarding the contributing mechanisms to subsidence in Louisiana. The outcome of this research is an improvement in the understanding of the spatial and temporal scales of subsidence as well as the driving mechanisms of subsidence. Overall, the greatest subsidence magnitudes are associated with anthropogenic activities, with the highest subsidence rates found in areas that are surrounded by levees, likely the result of peat auto compaction/degradation in desiccating areas. Other observable drivers of subsidence include coastal restoration project areas. In the observed time period, fluid withdrawal, the thickness of the Holocene and tectonic forces did not play a contributing role to the subsidence rates.

1. Rate variability and inherent error

The accreting basins at the Leonard Farm Site in Figure 24 show a significant discrepancy in elevation change rates. The cause of the apparent high accretion within the levees is likely an artifact of the high water level within the levees. The bright red appears to be Leonard's crawfish pond, which was most likely constructed between the two collection dates. The textured appearance of the area within the levees seems to be an artifact of the marsh terrain in the earlier dataset. The marsh was not present in the more recent 2015 Lidar dataset.

2. Near surface processes

Subsidence on and near levee systems typically involves fill compaction and loading effects, although some researchers have speculated that deeper processes such as faulting can play a role (Culpepper et al., 2019; Gagliano et al., 2003a; Törnqvist et al., 2008; USACE and IPET, 2009). Typically, Holocene sediment will compact initially at rates of $>10\text{mm/yr}$ during temporal ranges of 10^1 to 10^2 yrs. (spatial scale 10^1 m^2), but on the millennial scale, peat compaction rates average 5 mm/yr (Törnqvist et al., 2008). This implies that Holocene sediment compaction is a sizable contributor to local subsidence, wetland loss and RSLR (Törnqvist et al., 2008).

Levees are used to protect specific areas from moderate flooding in South Louisiana. Unfortunately, levees have other effects on the river basin including: causing a rise in flood stage, lessening channel capacity, and disconnecting the floodplain from the river and its tributaries (Alexander et al., 2012). Before significant engineering of the Mississippi River Basin began, annual flood events would bring new sediment and nutrients into the flood plain, rejuvenate nearby wetlands and restore riparian forests. (Yin and Nelson, 1996; Alexander et al. 2012; Galat et al., 1998; Dixon et al., 2010). The lower Mississippi River Basin current has more than 5,600 km of levees, which effectively cut-off 90 % of the delta plain from the river (Alexander et al., 2012; Mississippi River Commission, 2011).

Levees in South Louisiana are built from compacted sediment with impermeable clays positioned on the same side as the river to protect the integrity of the structure (Alexander et al., 2012; U.S.A.C.E, 2000). There are some questions regarding the sediments used and the amount of subsidence that the levee undergoes after construction (Dixon et al., 2006). Dixon (2006) proposed that levee failures during Hurricane Katrina could have been partially due to the integrity of substrate beneath the levee. The results of Dixon et al. (2006) suggested that the levee failure was related to more than a meter of subsidence, which had occurred since the levees were constructed.

Within certain levee systems, such as the CGGM, subsidence rates are slower than those of other levees, such as those just west of the Mississippi River (Figure 22). Subsidence rates within the CGGM vary from -30 to -5 mm/yr and in levees on the western shore of the Mississippi River, they range from -170 to -149 mm/yr . In the raw data, these areas of slower subsidence are notable for substantially lower elevations on the order of 5 m below sea level. The subsidence rates within levee systems may be slower than surrounding areas but without influx of new sediment from yearly floods, the elevation loss due to subsidence cannot be countered with accumulation. This causes a net negative effect over years and is the reason for lower elevations within established levee systems.

On the tens of kilometers scale, the subsidence rates within the CGGM levee are slower than those outside. Just east of Golden Meadow, there is increased subsidence (Figure 23). This could be due to the natural sediment compaction over time, activity of the Golden Meadow fault or fluid production.

Despite the unassuming subsidence rates within levee systems, it is clear this study corroborates the results of Dixon et al. (2010) and others, on the basis of the lower elevations of these leveed areas in the raw data maps. Levees, although a seemingly good first-line defense against storm surge and other threatening flooding events, have long-term impacts on the land they sequester from the hydrodynamic system of the delta.

3. Deep fluid withdrawal, oil and gas

Fluid withdrawal (spatial scale 10^1 - 10^3 m², temporal scale 10^1 - 10^3 yrs) can be an important cause of subsidence in many regions across the globe. Historically, there is a link between fluid withdrawal and subsidence in South Louisiana. Data from Galveston, TX and Grand Isle, LA suggests that there exists a temporal pattern in subsidence that is linked to the temporal pattern in fluid withdrawal (Kolker et. al, 2011). Three-quarters of the cumulative volume of hydrocarbons ever produced from Louisiana were extracted during a specific 17-year period (1964-1981) following which, Miller (2006) suggested that rates of subsidence increased to historical highs. From 1965 to 1993, subsidence rates were observed to range between 8 to 12 mm/year, however during the last 5000 years, Morton et al. (2005) suggested that rates were only 1 to 5 mm/year. It is important to recognize however that these variations in rates are fundamentally linked to the relative time frames of measurement (Morton et al., 2005).

The relationship between subsurface fluid production and subsidence is partially a function of geology of the aquifer or reservoir. For example, shallow reservoirs- such as most in onshore Louisiana drilling operations- might be expected to will cause less subsidence when produced than deeper, more compacted reservoirs. This is due to shallow reservoirs tending to be geopressed and more compressible (Carreon-Freyre, 2010; Goddard & Zimmerman, 2003). There also exists a lag time of about 10 years between production of a reservoir and land surface impacts such as subsidence (Morton et al., 2006; Barras et al., 2008; Morton et al. 2008).

In addition to fluid withdrawal causing reservoir or aquifer compaction, some have proposed that depressurization of reservoirs leads to fault motion within the subsurface (Morton and others: 2006, 2001). However, Olea and Coleman (2014) hold that local subsidence over a producing field should be a direct function of the production rate, causing subsidence to cease when production is complete. Using mathematical modeling, Mallman and Zoback (2007) found that only the subsidence immediately above the reservoir was accounted for and they could not reproduce the regional subsidence trends proposed by Morton et al., 2006 (Olea and Coleman, 2014).

The land surface over the Bully Camp salt dome has subsidence rates as high as -90 mm/yr, observed most often within marsh edge environments (Figures 18). In areas inundated with water the subsidence rate cannot be determined using Lidar data. The Clovelly salt dome - with subsidence rates about 20 mm/yr higher than Bully Camp in some places - may serve as an analog for what the subsidence rates over Bully Camp may have been previously.

Proximal to the Venice salt dome surface expression (Figure 20) many of the wells on the western side of the salt dome are situated in inundated canals and ponds. This makes it impossible to determine subsidence rates in their immediate vicinity.

Unfortunately, within the scope and methods of this study, it is impossible to determine if the apparent higher rates of land elevation loss over Bully Camp are due to marsh die off, fluid extraction, halokinetics or natural sediment compaction. In areas unaffected by possible salt motion, the results are varied. There can be no clear correlation between oil wells and the

subsidence rates over the time frame analyzed in this study. Even with specific production data from all the wells over a given salt dome, any correlations made regarding the relationship between fluid withdrawal and subsidence using these data would be challenged to differentiate between the causative roles of natural sediment compaction, halokinetics and fluid withdrawal.

4. Salt Domes

The study of salt domes, faulting and the effects of related processes on subsidence in South Louisiana remained largely underrepresented in the literature until recent years. Faulting has a significant effect on small-scale to regional subsidence within southeast Louisiana (spatial scale 10^1 to 10^3 m², temporal scale 10^1 to 10^5 yrs) Since the formation of the delta, rapid sediment accumulation, in conjunction with weak evaporite and shale horizons at depth has caused gravitational instability in the region and the facilitation of slippage (Dokka et al., 2006; Yuill et al., 2009). Because of the relative buoyancy of the sediment overlying low-density salt domes, much of Mississippi River Delta's underlying strata is tectonically unstable (Dokka et al., 2006; Törnqvist et al., 2008; Yuill et al., 2009). Regionally, Figure F.3.3 shows the suggested vertical and southward movement of the entire deltaic section south of Lake Pontchartrain as the underlying Louann salt serves as a ductile surface for slippage (Dokka et al., 2006).

Halokinesis causes variable local pressures within the subsurface, which can induce or amplify fault motion (Yuill et al., 2009). Additionally, salt diapirism causes radial fault zones to form, affecting local subsidence rates over 10^6 years and 10^3 to 10^5 m² (Diegel et al., 1995; Yuill et al., 2009). At least 15 of the 45 onshore salt domes in Louisiana have undergone the Frasch process of injecting heated water into the mine in order to extract sulfur (Olea et al., 2014). Many studies suggest that salt mining, salt migration and fault movement within the region cannot be ignored, though there have been few specific endeavors to understand the impacts these may have on local subsidence rates as of yet (Yuill et al., 2006 and refs therein; Dokka et al., 2006; Morton et al., 2005; Autin, 2002).

The Bully Camp salt dome underwent extensive sulfur mining in the 1960s and 70s (Morton et al., 2005). In addition, it has been a popular site for oil and gas production. Figure 33 shows the concentration of oil and gas wells over Bully Camp. The subsidence around the Bully Camp salt dome is of greater magnitude compared to other salt domes in the area such as Clovelly and Leeville. Although an increase in subsidence is clear, the proportion of that value which is due, if any, to oil and gas production, sulfur mining or halokinetics cannot be differentiated.

The Leeville salt dome is part of the Marchand-Timbalier-Calliou salt ridge-stock complex (presentation, Nancye H. Dawers). This area was also largely affected by sulfur mining in the early 20th century. Figure 21 shows oil and gas wells over the Leeville salt dome site. No trends in subsidence rates are apparent in these data for the Leeville salt dome.

The Clovelly salt dome site is notable for the increased concentration of canals and oil and gas production (Figure 18.). Similar to Leeville, there are no clear trends in subsidence rates that could be attributed to the tectonic action of this salt dome.

The Venice salt dome shows greater variance in surface elevation change (Figure 36). In the dome center accretion values exceed 116 to 236 mm/yr, but subsidence rates can exceed -94 mm/yr. Figure 20 shows the oil and gas activity around the dome. The location of this dome on the Birdsfoot delta may contribute to more active surface processes than the other salt domes evaluated in this study. Larger quantities of sediment influx would facilitate higher accretion

rates, whereas significant fault motion due to differential subsidence and oil and gas production might increase subsidence in the dome center.

Overall, there can be no conclusions on the correlation between salt dome location or activity and subsidence rates in this study. Given the temporal range of the data, it is likely the salt domes play an insignificant role in subsidence rates reflected in the final maps.

5. Thickness of the Holocene

Subsidence on or nearby a levee system involves near surface processes, specifically shallow subsidence. Near surface processes involve high rates of immediate subsidence, especially within peat layers. Peat horizons have been analyzed to determine the rate at which they compact. Typically, Holocene sediment will compact initially at rates of $>10\text{mm/yr}$ in the temporal ranges of 10^1 to 10^2 yrs (spatial scale 10^1 m^2), but on the millennial scale, peat compaction rates average 5 mm/yr (Törnqvist et al., 2008). This implies that Holocene sediment compaction is a sizable contributor to local subsidence, wetland loss and RSLR (Törnqvist et al., 2008).

In comparing the Holocene/Pleistocene Boundary Map (Figure 9) and the Instantaneous Slope Map (Figure 12), there is a possible correlation to be made between thicker Holocene strata - an artifact of the Terrebonne Trough - and an increased density of negative slope values in the south-central Terrebonne data. Though the subsidence map does not show greater magnitudes of elevation loss in this area, the negative slope values imply a greater variability in land surface elevation magnitudes. The increased Holocene thickness (more than 170 m) is also apparent near Leeville and the Birdsfoot (Figure 9). It has been established that Holocene deposits within the Mississippi River Delta there are subjected to subsidence due to their rapid deposition, lack of sufficient consolidation and slippage along weak stratigraphic horizons at depth (Dokka et al., 2006; Törnqvist et al., 2008; Yuill et al., 2009). The density of negative instantaneous slope values in south-central Terrebonne could result from other regional trends, such as an increase in natural sediment compaction in areas with thicker Holocene deposits or variations in vegetation between datasets.

In northern Terrebonne, there is an area of slightly lessened subsidence just south of Thibodaux that is congruent with a thinner Holocene (Figure 9). However, this area also has more infrastructure, including highway 90, so the link between these rates and Holocene thickness is not clear.

Unfortunately, the Holocene-Pleistocene comparison did not yield any other clear correlations with the remainder of the data. Given the temporal range of the data as 12 to 13 years, it follows that this variable would not play a large role in observed subsidence during this time. Additionally, the vertical resolution of the Holocene surface isopach exceeds 30.5 m (100 ft) in some areas, making the margin of error of these data orders of magnitude greater than the land elevation change rate values (see Figure 39 in Appendix B for precision values for these data).

B. ACCRETION

1. Coastal Protection Project Sites

Many coastal protection projects were started during the period of data collection (2002/3-2015). Their impacts were easily identifiable even at the hundreds of kilometers scale due to positive changes in land surface elevation. The projects resulted in an increase in land elevation in the tens to hundreds of mm/yr, starkly contrasting the surrounding areas that continued to subside.

The Little Lake Shoreline Protection and Marsh Creation Project involved the construction of dikes adjacent to the shoreline and marsh in-filling/creation. More than 2.34 km² (2,800,000 cubic yards) of dredged material were moved to create and elevation increase of 76.2 cm (2.5 ft) across 3.84 km² (950 acres) of marshland (based on NAVD 88 elevation). Along the Little Lake shoreline, 7,620 m (25,000 ft) of rock dike were built (Herbert Inc., 2014). The project was headed by CWPPRA and completed in 2007, about 8 years prior to the collection of the second Lidar dataset. Comparing the project site and surrounding areas, it is clear the project was successful in reversing the land loss that would have occurred along this southern cusp of Little Lake. Surpassing avoiding subsidence, this area is showing near uniform accretion (Figure 29b).

Like the Little Lake project, the Barataria Barrier Island Complex Project: Pelican Island and Pass La Mer to Chaland Pass project was multi-faceted (Figure 30b). It included beach in-filling, the building of dunes and berms, and the creation of a back-barrier marsh platform (Montiano, 2004). About three years passed between the completion of this project and the collection of the final Lidar dataset in 2015. Over this time, the project's success is still apparent on the Chaland headland and Pelican Island. In some areas there is apparent accretion of 87 mm/yr or more. Subsidence rates exceeding -107 mm/yr are apparent on the western shore near Bay Long, an area not included in the project.

The West Lake Boudreaux Shoreline Protection and Marsh Creation Project (West Lake Boudreaux, 2007) involved the creation of 1.15 km² (284 acres) of marsh from dredged material and the construction of 3,962.4 m (13,000 ft) of rock dike (Figure 31b). Construction was completed in 2009 but positive vertical change values exceed 50 mm/yr in various areas of the project.

Each of these projects have similar construction outlines and comparable success rates. All of these projects involved the influx of new sediment to the project area and construction of some form of infrastructure to retain the material. The Little Lake Shoreline Project was completed the earliest of the three analyzed (2007) but the positive land elevation change in the more recent project areas is still significant. These project sites represent some of the most pronounced change in elevation rates within the study area and time.

2. Accretion associated with sediment transport from the Mississippi River

The notable high accretion rates near wells on the northeastern side of the Venice salt dome could be the result of greater accretion due to the influx of sediment coming from the river (Figure 20). This is probable given the direction of flow coming from the river, supplying new sediment continuously. This could also be the result of infrastructure built around the wells to support production. This seems to indicate that it is possible for accretion to outpace fluid withdrawal-related subsidence, if it exists, in dynamic areas as this.

C. Erosion

While not a primary focus of this study, the results presented here show examples of erosion across the study region. The largest magnitude of erosion appears to be anthropogenic scour associated with levee construction. One particular example of this is Figure 19, which is located at the Leonard's Farm site where new levees had been constructed between the two data collection periods. Erosion rates here may be estimated to exceed -170 mm/yr across a kilometer and ~ 20 m² area. Another example of erosion appears at marsh edges that were likely impacted by waves (Figures 14 and 25). Figure 14 shows marsh edge loss on the shore of Little Lake. Erosion rates here may exceed -94 mm/yr, over a spatial area of hundreds of kilometers long and covering tens of square kilometers.

D. Instantaneous Slope

One way to distinguish between potential drivers of land elevation change is by examining the instantaneous slope. In the analysis of instantaneous slope, the differenced value of the LOSCO 2002/3 slope and USGS 2015 data set's slope was determined for the study region. When the "Slope" function was used on the 2002/3 and 2015 datasets, the output raster of each showed the elevation variability in the study area based on the elevation magnitude of the point in the data set, and those points immediately adjacent to it. Each point is a 5x5m area and the instantaneous slope function compares one cell to the surrounding eight cells, making up a 15 x 15m area. A high slope value in the output raster corresponds to a large variability in elevation of the area. A fixed area that contains a curb with a drop off of ~6 inches would have a higher instantaneous slope value than the side of a hill with a gradual slope. A low value in the output raster corresponds to low variability of elevations in the area. An area that is more smooth, such as a parking lot or beach, will have a much lower instantaneous slope value than marshland or forest. After evaluating the instantaneous slope sets 2002/3 and 2015 individually, the sets were subtracted to determine the slope over time. The 2015 data was subtracted from the 2002 data.

The resulting map, Figure 12, shows highly positive values, highly negative values, and areas close to zero. Positive values corresponded to a high degree of variability in elevation in 2002 that lessened in the same area in 2015. In this scenario, land appears to have undergone a smoothing effect in the highly positive areas. This may occur in inundated areas if water level is higher in the later dataset, or it can occur as a result of vegetation loss.

For example, on the shores of Little Lake, the positive slope values parallel the shorelines of bays, which suggests there was a larger, positive slope previously due to the presence of marsh, but now there is no slope due to wetland loss (Figures 14 and 14b). Due to the location of this change, the mechanism of wetland loss is likely erosion. Marsh edge loss due to die-off, saltwater intrusion or a difference in water level between the differenced Lidar collection dates is clearly denoted by positive slope values (Figure 14).

Negative values corresponded with a low degree of variability in elevation in 2002 and a high degree of elevation variability in 2015. A good example of this would be new construction such as buildings or levees (Figure 15) or new construction in Port Fourchon (Figure 16). Areas converted from water to marshlands would show negative values as well. An example of this is the negative slope values clustered in central-southwestern Terrebonne (Figure 12). Lidar data in this region may have been shot later in the year - possibly in March - which could mean there is

more vegetation in this region in the 2015 data (2002/3 data may have been shot January/February). This could cause more negative slope values in the final map.

Alternatively, it is possible that such a broad area showing negative values implies regional forces are the cause of land surface elevation change. There could be tectonic activity in this region and is a potential contributing factor to these observations (Armstrong et al., 2014; Dokka, 2006; Gagliano et al., 2003b, Kuecher & Roberts, 2001; McCulloh and Heinrich, 2012; Wallace, 1962; Morton et al., 2005; and Culpepper et al., 2019).

The CGGM levee system shows a slightly higher concentration of negative values within the levee perimeter (Figure 13). This affirms that levees could be contributing to subsidence inside their bounds. This process would cause a non-uniform consolidation of sediment such that variability in elevations would be greater. Overtime, sediments deposited on a land surface will compact by expelling water from the pore space between grains (Törnqvist et al., 2008). With a lack of influx of sediment from annual floods, the accommodation on the compacting land surface cannot be infilled with new sediment, causing a net loss in land elevation. Outside of the levee, erosional and depositional forces are prominent causes of vertical loss as shown by the greater number of positive slope values.

Near Triumph, just west of Fort St. Philip, there is a greater concentration of negative slope values (Figure 15). These negative values mean there is more variability in the elevations of the land surface in this area. This could mean the area is being converted to marsh. More positive values in this region indicate land or marsh loss due to die off, or water inundation.

There were also areas with no change from 2002 to 2015. These areas showed no change in variability magnitude over the specified time. These areas would be estimated to be undergoing the same geological processes during the time period.

Utilizing instantaneous slope with Lidar data can prove useful when following the progress of Coastal Restoration Projects and areas of interest for future projects. Within the Little Lake Shoreline Protection and Marsh Creation Project area, uniform positive and negative values indicating that the accretion occurring there is occurring relatively uniformly throughout the project area. Using this tool, one can see if change is occurring where expected and possibly predict the type of changes occurring.

V. Conclusion

A combination of spatial elevation datasets and GIS layers of geologic and anthropogenic features were compared against each other to assess the patterns of subsidence within southeast Louisiana and the function of various factors involved in land surface changes.

A fundamental result of this effort was the development of spatial and temporal datasets that provide a better understanding of the spatial and temporal distribution of subsidence patterns as well as insight to the causative mechanisms of subsidence. There were four primary results of this effort: 1) Areas with thicker Holocene deposits do not clearly correlate to higher subsidence rates suggesting natural sediment compaction may not play a significant role in land elevation loss on a decade scale, or data was insufficiently precise 2) Levees and coastal restoration projects have a clear effect on subsidence within the given time period, 3) Salt motion, halokinetics, and tectonics do not have an obvious effect on subsidence rates on a decadal scale, 4) Fluid extraction does not have a clear effect on subsidence on a decade or kilometer scale, but

may have a role at a spatial scale of meters during monthly to annual time frames, instead of decades.

A secondary objective of this study was to determine if Lidar data allowed for more accurate and precise values of subsidence on a decade scale, which it did. Additionally, an effort was made to use instantaneous slope analysis as a way to measure land elevation change processes and determine its potential use in similar studies in future.

The hypothesis that natural sediment compaction and levees were significant contributors to subsidence over decades and tens of kilometers was correct. However, regional faulting and fluid extraction proved to be less influential over the observed temporal and spatial parameters of the study. Faulting likely plays a much larger role on the hundreds to thousands of years scale. Fluid withdrawal would be a more focused issue on the 10^{-1} - 10^2 scale and during months to years but no clear indication emerges from this study.

VI. References

- Alexander, J.S., Wilson, R.C., & Green, W.R. (2012). A brief history and summary of the effects of river engineering and dams on the Mississippi River system and delta: U.S. Geological Survey Circular 1375, pg. 43.
- Armstrong, C., Mohrig, D., Hess, T., George, T., & K. Straub (2014). Influence of growth faults on coastal fluvial systems: Examples from the late Miocene to Recent Mississippi River Delta: *Sedimentary Geology*, v. 301, p. 120-132.
- Autin, W. J. (2002). Landscape evolution of the Five Islands of south Louisiana: scientific policy and salt dome utilization and management, *Geomorphology*, 47, p. 227-244.
- Barras, J.A., Bourgeois, P.E., & Handley, L.R. (1994). Land loss in coastal Louisiana 1956-90: National Biological Survey, National Wetlands Research Center Open File Report 94-01, p. 4.
- Barras, J.A., Beville, S., Britsch, D., Hartley, S., & Hawes, S. (2003). Historical and projected coastal Louisiana land changes: 1978–2050. Open File Rep. 03-334, US Geol. Surv., Washington, DC. (Cover Image)
- Blum, M.D., & Roberts, H.H. (2012). The Mississippi Delta Region: Past, Present, and Future; *Annual Review of Earth and Planetary Sciences*, v. 40, p. 655-683.
- Cahoon, D. R., Lynch, J. C., Perez, B. C., Segura, B., Holland, R. D., Stelly, C., & Hensel, P., (2002). High-precision measurements of wetland sediment elevation; II, The rod surface elevation table: *Journal Of Sedimentary Research*, v.72, no. 5, p. 734-739.
- Carreon-Freyre, D.C. (2010). Land subsidence processes and associated ground fracturing in central Mexico: IAHS-AISH Publication, v. 339, p. 149-157.
- Coastal Protection and Restoration Authority (CPRA) of Louisiana (2017). Coastwide Reference Monitoring System-Wetlands Monitoring Data. Retrieved from Coastal Information Management System (CIMS) database. <http://cims.coastal.louisiana.gov>. Accessed 25 January 2017.
- Coleman, J.M., Roberts, H. H., & Stone, G.W. (1998). Mississippi River Delta: An Overview: *Journal of Coastal Research*, v. 14, n. 3, p. 698-716.
- Conner, W.H., & Day, J.W. (1987). The ecology of Barataria Basin Louisiana: an estuarine profile, U.S. Fish Wilfl. Serv. Biol. Rep., 85, 7.13, 165pp.
- Couvillion, B.R., Barras, J.A., Steyer, G.D., Sleavin, W., Fischer, M., Beck, H., Trahan, N.; Griffin, B., & Heckman, D. (2011). Land Area Change in Coastal Louisiana from 1932 to 2010: U.S. Geological Survey Scientific Investigations Map 3164, scale 1:265,000, pamphlet, 12p.

Culpepper, D. McDade, E. C. Dawers, N., Kulp, M. & Zhang, R. (2019). "Synthesis of Fault Traces in SE Louisiana Relative to Infrastructure," Publications. 30. <https://digitalcommons.lsu.edu/transet_pubs/30>.

Cunningham R., Gisclair D., & Craig J. (2004). The Louisiana statewide LiDAR project. http://atlas.lsu.edu/central/la_LiDAR_project.pdf (Accessed 5 November 2015).

Data distributed by "Atlas: The Louisiana Statewide GIS." LSU Geography and Anthropology, Baton Rouge, LA (2007). <<http://atlas.lsu.edu>>.

Dawers, N. H. Presentation, 4 May 2017. Slide 2-25.

DeLaune, R.D., & Pezeshki, S.R. (1994). The Influence of Subsidence and Saltwater Intrusion on Coastal Marsh Stability: Louisiana Gulf Coast, U.S.A.: *Journal of Coastal Research*, v. Special Issue, no. 2, p.77-89.

de Zeeuw-van Dalfsen, E., Pedersen, R., Hooper, A., & Sigmundsson, F. (2012). Subsidence of Askja Caldera 2000-2009; modeling of deformation processes at an extensional plate boundary, constrained by time series InSAR analysis: *Journal Of Volcanology And Geothermal Research*, v. 213-214, p. 72-82.

Diegel, F. A., J. F. Karlo, D. C. Schuster & R. C. Shoup (1995). Cenozoic structural evolution and tectono-stratigraphic framework in the northern Gulf Coast continental margin: *AAPG Memoir*, v. 65, p. 109–151.

Dixon, T.H., Amelung, F., Ferretti, A., Novali, F., Rocca, F., Dokka, R., Sella, G., Kim, S.W., Wdowinski, S., & Whitman, D. (2006). Subsidence and Flooding in New Orleans: *Nature*, v. 441, p. 587-588.

Dokka, R.K. (2006). Modern-day Tectonic subsidence in coastal Louisiana: *Geology*, v. 34, p. 281-284.

Dokka, R.K., Sella, G.F., & Dixon, T.H. (2006). Tectonic control of subsidence and southward displacement of southeast Louisiana with respect to stable North America: *Geophysical Research Letters*, v. 33, L23308.

Dokka, R.K. (2008). A Comparison of Geologic and Geodetic Measurement Methods Used to Quantify 20th Century Subsidence of the Louisiana Coast: *Geological Society of America Abstracts with Programs*, v. 40, no. 6, p. 261.

Douglas, B.C. (2001). Sea level change in the era of the recording tide gauge, *Sea Level Rise: History and Consequences: International Geophysical Series*, vol. 75, p. 37–64.

Gagliano, S.M., Kemp, E.B. III, Wicker, K.M. & Wiltenmuth, K.S. (2003a). Active Geological Faults and Land Change in Southeastern Louisiana: A Study of the Contribution of Faulting Relative Subsidence Rates, Land Loss and Resulting Effects on Flood Control, Navigation, Hurricane Protection and Coastal Restoration Projects: U.S. Army Corps of Engineers, Contract No. DACW 29-00-C-0034.

Gagliano, S.M., Kemp, E.B. III, Wicker, K.M., Wiltenmuth, K.S., & Sabate, R.W. (2003b). Neotectonic framework of southeast Louisiana and applications to coastal restoration: Transactions of the 53rd Annual Conference of the Gulf Coast Association of Geological Societies and the Gulf Coast Section SEPM 2003, Baton rouge, LA, October 22-24, 2003, v. 53, p. 262–272.

Goddard, D.A., & Zimmerman, R.K. (2003). Shallow Miocene and Oligocene Gas Potential: Southeastern Louisiana's Florida Parishes: GCAGS/GCSSEPM Transactions, v. 53, p. 287-301.

Greensmith J.T., & Tucker E.V. (1986). Compaction and consolidation. In: van de Plassche O. (eds) Sea-Level Research. Springer, Dordrecht.

Heinrich, P., Paulsell, R., Milner, R., Snead, J. & Peele, H. (2015). Investigation and GIS development of the buried Holocene-Pleistocene surface in the Louisiana coastal plain: Baton Rouge, LA, Louisiana Geological Survey-Louisiana State University for Coastal Protection and Restoration Authority of Louisiana, 140 p., 3 pls.

Herbert, M. P. Inc.. "Little Lake Shoreline Protection and Marsh Creation Project (BA-37)." Coastal Protection and Restoration Authority of Louisiana. (2014) Post-Construction Survey Monitoring Report; <[https://www.lacoast.gov/reports/project/Little_Lake_\(BA-37\)_Post_Construction_Survey_Report_2013.pdf](https://www.lacoast.gov/reports/project/Little_Lake_(BA-37)_Post_Construction_Survey_Report_2013.pdf)>.

Kesel, R.H. (1988). The Decline in the Suspended Load in the Lower Mississippi River and its influence on Adjacent Wetlands: Environmental Geology and Water Sciences, v. 11, no. 3, p. 271-281.

Kolker, A.S., Allison, M.A., & Hameed, S. (2011). An evaluation of subsidence rates and sea-level variability in the northern Gulf of Mexico: Geophysical Research Letters, v. 38, L21404.

Kosters, E.C., & Suter, J.R. (1993). Facies Relationships and Systems Tracts in the Late Holocene Mississippi Delta Plain: Journal of Sedimentary Petrology, v. 63, n. 4, p. 727-733.

Kuecher, G. J. & Roberts H. (2001). Evidence of active growth faulting in the Terrebonne Delta Plain, South Louisiana: Implications for wetland loss and the vertical migration of petroleum. Environmental Geosciences, Vol. 8, pp 77-94.

Kulp, M., & Howell, P.D. (1998). Assessing the accuracy of Holocene subsidence rates in southern Louisiana as indicated by radiocarbon-dated peats: Geological Society of America Abstracts with Programs, v. 30 p. 142.

Kulp, M. (2000). Holocene Stratigraphy, History, and Subsidence of the Mississippi River Delta Region, North-Central Gulf of Mexico: PH.D. thesis, University of Kentucky, Lexington, Department of Geological Sciences.

“Little Lake Shoreline Protection/Dedicated Dredging Near Round Lake (BA-37).” Louisiana Coastal Wetlands Conservation and Restoration Task Force. Report. Sept 2015. <<https://www.lacoast.gov/reports/gpfs/BA-37.pdf>>.

Louisiana Coastal Area (LCA), (2005). Louisiana Coastal Area, Louisiana: Ecosystem Restoration Study. U.S. Army Corps of Engineers, New Orleans District.

Louisiana Coastal Wetlands Restoration and Conservation Task Force (LCWRCTF) (1993). Louisiana Coastal Restoration Plan-Terrebonne Basin, Appendix E, Website. <http://www.lacoast.gov/reports/CWCRP/1993/TerreApndxE.pdf>

McCulloh, R.P. & P.V. Heinrich (2012). “Surface faults of the south Louisiana growthfault province”. In Recent Advances in North American Paleoseismology and Neotectonics east of the Rockies and Use of the Data in Risk Assessment and Policy, Geological Society of America Special Paper, No. 493, pp. 37-49, doi:10.1130/2012.2493(03).

Miller, B. (2006). Hydrocarbon Production, Surface Subsidence and Land Loss in Louisiana: Gulf Coast Association of Geological Societies Transactions, v. 56, p.579-589.

Montanio, P.A. “Barataria Plaquemines Barrier Island Complex Project, CWPPRA project fed. no. BA-38, Pass la Mer to Chalant Pass and Pelican Island environmental assessment, Plaquemines Parish, Louisiana”. (2004). Professional Paper. <<https://repository.library.noaa.gov/view/noaa/4090>>.

Morton, R.A., Bernier, J.C., Barras, J.A., & Ferina, N.F. (2005). Historical Subsidence and Wetland Loss in the Mississippi Delta Plain: Gulf Coast Association of Geological Societies Transactions, v. 55, p. 555-571.

Morton, R.A., Bernier, J.C., & Kelso, K.W. (2009). Recent subsidence and erosion at diverse wetland sites in the southeastern Mississippi delta plain: U.S. Geological Survey Open-File Report, 2009–1158, v. 39, p. 41-221.

Morton, R. A., Buster, N. A., & Krohn, M. D. (2002). Subsurface controls on historical subsidence rates and associated wetland loss in southcentral Louisiana: Transactions Gulf Coast Association of Geological Societies, v. 52, p. 767-778.

Morton, R. A., Bernier, J.C., Barras, J.A., & Ferina, N.F. (2005). Rapid Subsidence and Historical Wetland Loss in the Mississippi Delta Plain: Likely Causes and Future Implications, U.S. Geological Surveys, Open File Report, p. 3-38.

Morton, R.A., Tiling, G., & Ferina, N.F. (2003). Causes of hot-spot wetland loss in the Mississippi delta plain; Environmental Geosciences, v. 10, n. 2, p. 71-80.

- Nelson, S.A.C., Soranno, P.A., & Qi, J. (2002). Land-Cover Change in Upper Barataria Basin Estuary, Louisiana, 1972-1992: Increases in Wetland Area: *Environmental Management*, 2002, v. 29, n. 5, p. 716-727.
- Olea, R.A., & Coleman Jr., J.L. (2014). Synoptic Examination of Causes of Land Loss in Southern Louisiana as They Relate to the Exploitation of Subsurface Geologic Resources: *Journal of Coastal Research*, v. 30, no. 5, p. 1025-1044.
- Penland, S., & Ramsey, K.E. (1990). Relative sea-level rise in Louisiana and the Gulf of Mexico: *Journal of Coastal Research*, v. 6, p. 323-342.
- Penland, S. (1988). Transgressive depositional systems of the Mississippi Delta plain; a model for barrier shoreline and shelf sand development: *Journal of Sedimentary Petrology*, v. 58, no. 6, p. 932-949.
- Pfeffer, J., & Allemand, P. (2016). The key role of vertical land motions in coastal sea level variations: A global synthesis of multisatellite altimetry, tide gauge data and GPS measurements: *Earth and Planetary Science Letters*, v. 439, p. 39-47.
- Reed, D.J., & Yuill, B. (2009). Understanding Subsidence in Coastal Louisiana: http://www.lacoastpost.com/UNO_SubsidenceinLA_09.pdf (Accessed October 22, 2016).
- Roberts, H.H., Bailey, A., & Kuecher, G.J. (1994). Subsidence in the Mississippi River delta – Important influences of valley filling by cyclic deposition, primary consolidation phenomena, and early diagenesis: *Transactions, Gulf Coast Association of Geological Societies*, v. 44, p. 619-629.
- Roberts, H.H., & Coleman, J.M. (1996). Holocene Evolution of the deltaic plain: a perspective – From Fisk to present: *Engineering Geology*, v. 45, p. 113-138.
- Roberts, H.H. (1997). Dynamic Changes of the Holocene Mississippi River Delta Plain: The Delta Cycle: *Journal of Coastal Research*, v. 13, no. 3, p. 605-627.
- SONRIS database. Accessed Oct 2016. Well Status Information. <http://sonris-www.dnr.state.la.us/www_root/launch_java.html?fmx=SRCN0210.fmx.end>.
- Shinkle, K.D., & Dokka, R.K. (2004). Rates of Vertical Displacement at Benchmarks in the Lower Mississippi Valley and the Northern Gulf Coast: NOAA Technical Report, NOS/NGS 50.
- Törnqvist, T.E., Wallace, D.J., Storms, J.E.A., Wallinga, J., Van Dam, Remke, Blaauw, M., Derksen, M.S., Klerks, C.J.W., Meijneken, C., & Snijders, E.M.A. (2008) Mississippi Delta subsidence primarily caused by compaction of Holocene strata: *Nature*, v. 1, p. 172-176.
- Törnqvist, T.E., González, J.L., Newsom, L.A., van der Borg, K., de Jong, A. F. M., & Kurnik, C.W. (2012). Deciphering Holocene sea-level history on the U.S. Gulf Coast: A high-resolution

record from the Mississippi Delta: Geological Society of America Bulletin, v.116, no. 7-8, p. 1026-1039.

U.S. Army Corps of Engineers. Interagency Performance Evaluation Task Force (2009). Performance Evaluation of the New Orleans and Southeast Louisiana Hurricane Protection System Final Report of the Interagency Performance Evaluation Task Force. Retrieved from <https://biotech.law.lsu.edu/katrina/ipet/Volume%20I%20FINAL%2023Jun09%20mh.pdf>

Wallace, W. E. (1962). Fault map of south Louisiana. Transactions Gulf Coast Association Geological Societies, Vol. 12, p. 194.

“West Lake Boudreaux Shoreline Protection and Marsh Creation (TE-46).” Louisiana Coastal Wetlands Conservation and Restoration Task Force. Report. Sept 2007. <<https://www.lacoast.gov/reports/gpfs/TE-46.pdf>>.

Yu, S.Y., Törnqvist, T.E. & Hu, P. (2012). Quantifying Holocene lithospheric subsidence rates underneath the Mississippi Delta: Earth and Planetary Science Letters, 331-332, p. 21-30.

Yuill, B., Lavoie, D., & Reed, D.J. (2009). Understanding Subsidence Processes in Coastal Louisiana, Journal of Coastal Research, v. 54, p. 23-36.

Zou, L., Kent, J., Lam, N., Cai, H., Qiang, Y., & Li, K. (2015). Evaluating Land Subsidence Rates and Their Implications for Land Loss in the Lower Mississippi River Basin: Water, v. 8, n. 10, p. 1-15.

VII. Appendix A: Tables

Table 1: LIDAR Datasets

Dataset	Acquisition dates	Acquisition dates within study area	Spatial resolution	Horizontal Datum	Vertical Datum	GEOID	Pixel Depth/ radiometric res	Precision Shot	Pulse and NPS units	Number of bands
Losco_2002/3	1999-2008	2002/2003	5 m	UTM Zone 15 N meters, NAD 83 (GRS80)	NAD83, NAVD88 ft	GEOID99	32 bit	Vert. acc.: 6 - 12 in Horiz.: 3-6 ft	N/A	1
USGS_Bara_2013	March 2013	March 2013	2 m	UTM Zone 15 N meters	NAD83	GEOID12A	32 bit	3 decimal places (mm)	m	1
USGS_NBara_2013	March 2013	March 2013	1 m	UTM Zone 15 N meters	NAD83	GEOID12A	32 bit	3 decimal places (mm)	m	1
USGS_Terrace_2015	2015	2015, Revised Dec 2016	1 m	UTM Zone 15 N meters	NAD83	GEOID12A	32 bit	3 decimal places (mm)	m	1

Table 2: Ancillary Data Sources

Dataset	Source	Specs
Holocene_Pleistocene Raster	CPRA	Data Type: Raster Resolution: 100 m ² Z range: -310.70- 498.36 m Datum: NAVD88 Compiled 2013
Oil & Gas Wells	LDNR public access SONRIS database, Office of Conservation	Data Type: Point File Display: All wells permitted by the State
Injection Wells	LDNR public access SONRIS database	Data Type: Shapefile
Levees	LDNR public access SONRIS database	Data Type: Shapefile GCS_North_American_1983 Linear Unit: Meter (1.000000) NAD_1983_UTM_Zone_15N DATUM: D_North_American_1983 PROJECTION: Transverse_Mercator
Salt Domes	N Dawers (pers. comm) C. McLindon (pers.comm)	
Coastal Protection and Restoration Project Sites	Coastal Protection and Restoration Authority of Louisiana (CPRA) and the USGS National Wetland Research Center via LDNR	Datum: NAVD88 “Contains polygon features for infrastructure associated with CPRA coastal protection and coastal restoration projects. These features include but are not limited to borrow sites, marsh creation, marsh nourishment, fill areas, and dunes.”

	public access SONRIS database	
2007 Louisiana Coastal Marsh-Vegetative Type Map of the Louisiana Coastal Marsh-Vegetative Type Database	Louisiana Department of Wildlife and Fisheries, Fur and Refuge Division, LSU AgCenter, and U.S. Geological Survey's National Wetlands Research Center	Data Type: Vector Line The original data set was collected through visual field observation by Charles Sasser and Jennke Visser of LSU. The observations were made while flying over the study area (Louisiana Coastal Zone) in a Bell 206 Jet Ranger helicopter. Flight was along north/south transects spaced 1.87 miles apart from the Texas State line to the Mississippi State line. Vegetative data was obtained at pre-determined stations spaced at 0.5 miles along each transect. The stations were located using a Trimble Ag 122 Global Positioning System (GPS) and a computer running ArcGIS. This information was recorded manually into field tally sheets and later this information was entered into a Microsoft Access database. At this point, this information was brought into a GIS application by converting the file to a database format (dbf). The marsh type delineation lines were produced by freehanding contours through on-screen interpretation. The flight line data was used as a guide for drawing the lines. The new data set resulted in a line coverage delineating vegetative marsh types.

Table 3: Composition of Created Maps

Map	Data Sources Used
Holocene Thickness from Losco_Bara_2002/3 Surface	Losco_Bara_2002/3
	USGS_Bara_2013
	USGS_Terre_2015
	Holocene_Pleistocene Raster
Depth to Holocene-Pleistocene Boundary (Holocene Thickness from USGS_Bara_2013/USGS_Terre_2015 Surface)	Losco_Bara_2002/3
	USGS_Bara_2013
	USGS_Terre_2015
Instantaneous Slope	Losco_Bara_2002/3
	USGS_Bara_2013
	USGS_Terre_2015
Lidar Difference Map/ Subsidence Map	Losco_Bara_2002/3
	USGS_Bara_2013

VIII. Appendix B: Supplemental Images

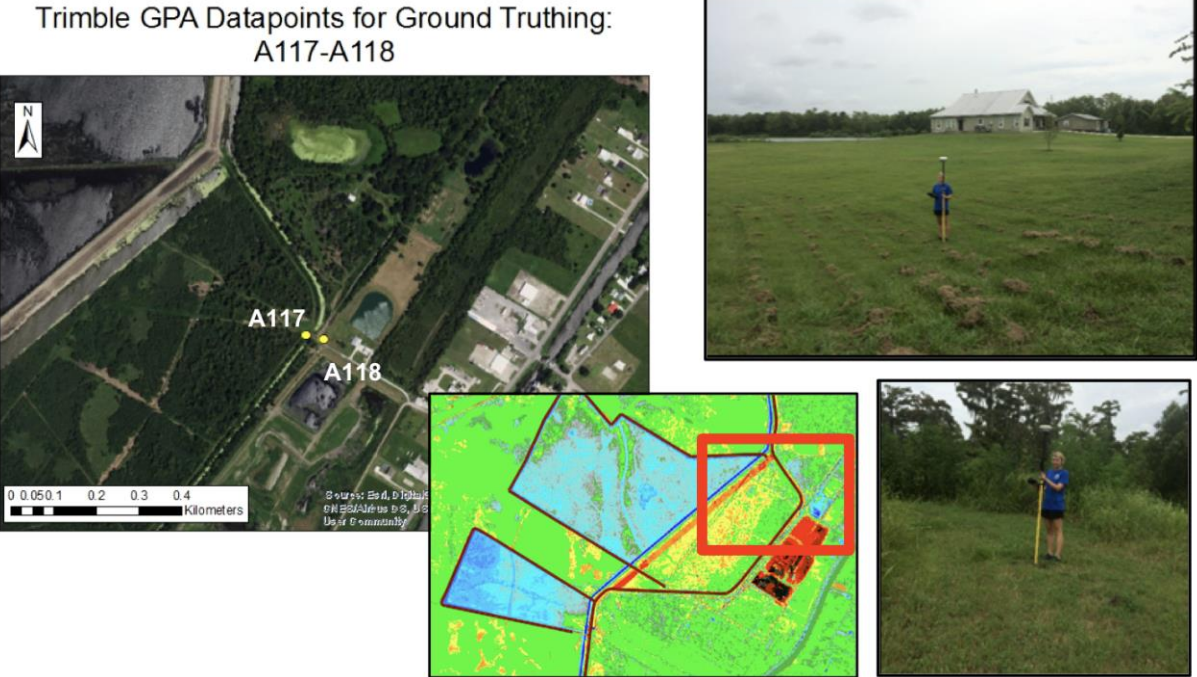


Figure 37: Fieldwork completed near Leonard’s Farm site; RTK values A117-A118.

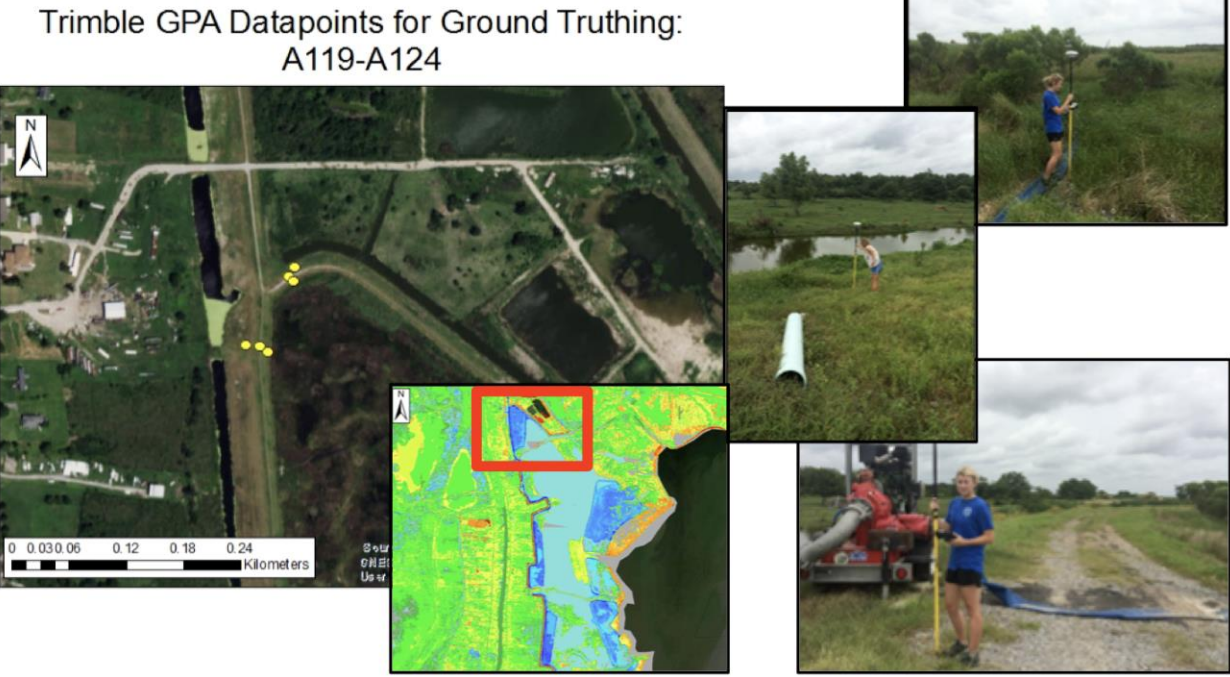


Figure 38: Fieldwork completed near the West Lake Boudreaux Shoreline Protection and Marsh Creation Project. The pumping of the pastured area appears to have caused significant subsidence in a short period of time. RTK values A119-A124.

RTK values A119-A124.

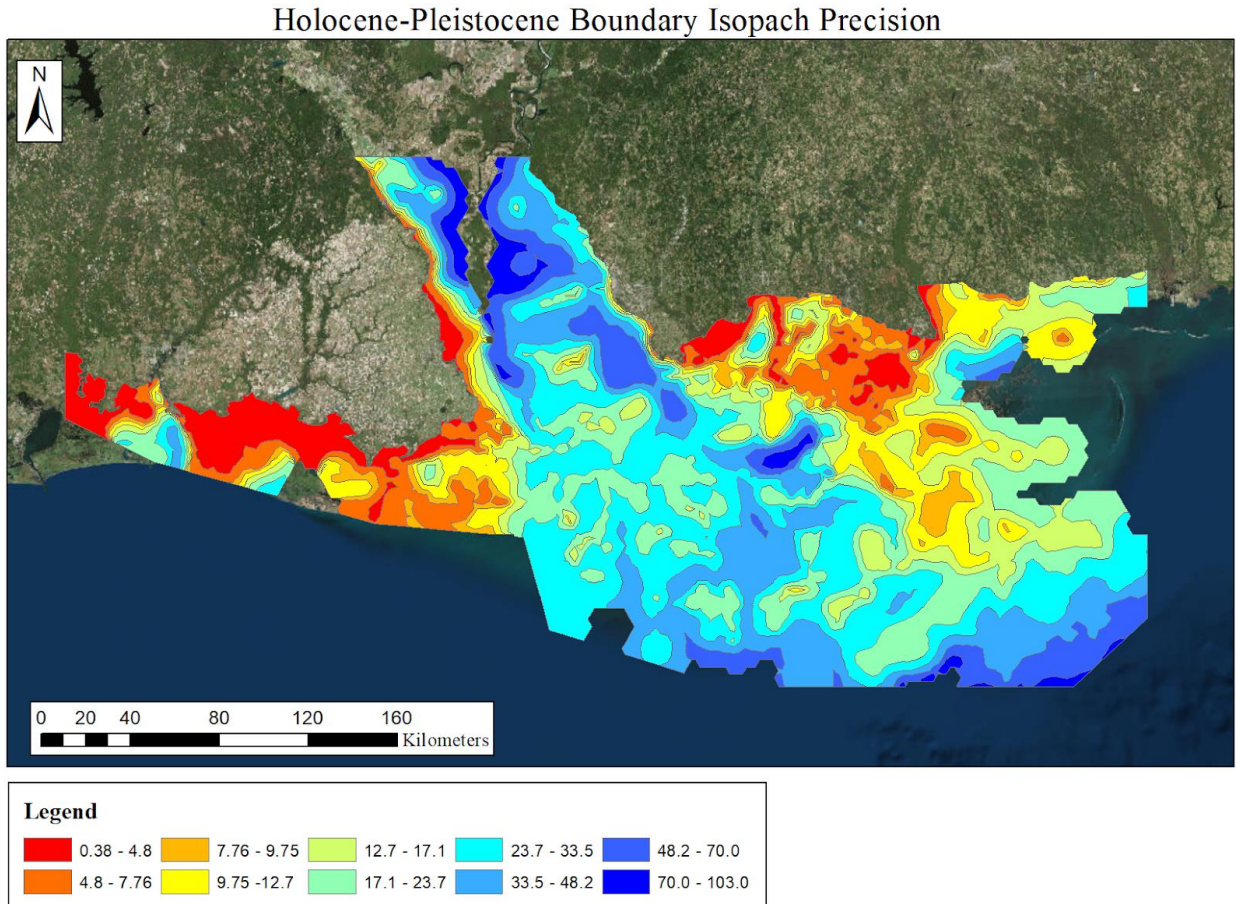


Figure 39: Precision Map of Holocene-Pleistocene Boundary Isopach; cooler colors indicate lower precision due to lack of data or poor data integrity.

IX. Vita

The author was born in Houston, Texas. She obtained her Bachelor's degree in Geology from the University of Alabama in 2015. She joined the University of New Orleans Earth and Environmental Science graduate program to pursue a Masters in Earth and Environmental Science and became a member of Dr. Mark Kulp and Dr. Alex Kolker's research groups in August of 2015.